Molecular Structures, Vibrational Spectroscopy, and Normal-Mode Analysis of $M_2(C{\equiv}CR)_4(PMe_3)_4$ Dimetallatetraynes. Observation of Strongly Mixed Metal−Metal and Metal−Ligand Vibrational Modes

Kevin D. John,[†] Vincent M. Miskowski,[†] Michael A. Vance,[‡] Richard F. Dallinger,[‡] Louis C. Wang,[†,§] Steven J. Geib,[†] and Michael D. Hopkins*[,†]

Departments of Chemistry, University of Pittsburgh, Pittsburgh, Pennsylvania 15260, and Wabash College, Crawfordsville, Indiana 47933

Received July 23, 1998

The nature of the skeletal vibrational modes of complexes of the type $M_2(C{\equiv}CR)_4(PMe_3)_4$ (M = Mo, W; R = H, Me, Bu^t, $SiMe_3$) has been deduced. Metrical data from X-ray crystallographic studies of $Mo_2(C{\equiv}CR)_4(PMe_3)_4$ (R = Me, Bu^t, $SiMe_3$) and $W_2(C{\equiv}CMe)_4(PMe_3)_4$ reveal that the core bond distances and angles are within normal ranges and do not differ in a statistically significant way as a function of the alkynyl substituent, indicating that their associated force constants should be similarly invariant among these compounds. The crystal structures of $Mo_2(C{\equiv}CSiMe_3)_4(PMe_3)_4$ and $Mo_2(C{\equiv}CBu^t)_4(PMe_3)_4$ are complicated by 3-fold disorder of the Mo_2 unit within apparently ordered ligand arrays. Resonance-Raman spectra ($^1(\delta{\rightarrow}\delta^*)$ excitation, THF solution) of $Mo_2(C{\equiv}CSiMe_3)_4(PMe_3)_4$ and its isotopomers (PMe_3-d_9, $C{\equiv}CSiMe_3$-d_9, $^{13}C{\equiv}^{13}CSiMe_3$) exhibit resonance-enhanced bands due to a_1-symmetry fundamentals (ν_a = 362, ν_b = 397, ν_c = 254 cm^{-1} for the natural-abundance complex) and their overtones and combinations. The frequencies and relative intensities of the fundamentals are highly sensitive to isotopic substitution of the $C{\equiv}CSiMe_3$ ligands, but are insensitive to deuteration of the PMe_3 ligands. Nonresonance-Raman spectra (FT-Raman, 1064 nm excitation, crystalline samples) for the $Mo_2(C{\equiv}CSiMe_3)_4(PMe_3)_4$ compounds and for $Mo_2(C{\equiv}CR)_4(PMe_3)_4$ (R = H, D, Me, Bu^t, $SiMe_3$) and $W_2(C{\equiv}CMe)_4(PMe_3)_4$ exhibit ν_a, ν_b, and ν_c and numerous bands due to alkynyl- and phosphine-localized modes, the latter of which are assigned by comparisons to FT-Raman spectra of $Mo_2X_4L_4$ (X = Cl, Br, I; L = PMe_3, PMe_3-d_9)$_4$ and $Mo_2Cl_4(AsMe_3)_4$. Valence force-field normal-coordinate calculations on the model compound $Mo_2(C{\equiv}CH)_4P_4$, using core force constants transferred from a calculation on $Mo_2Cl_4P_4$, show that ν_a, ν_b, and ν_c arise from modes of strongly mixed $\nu(Mo_2)$, ν(MoC), and λ(MoCC) character. The relative intensities of the resonance-Raman bands due to ν_a, ν_b, and ν_c reflect, at least in part, their $\nu(M_2)$ character. In contrast, the force field shows that mixing of $\nu(M_2)$ and $\nu(C{\equiv}C)$ is negligible. The three-mode mixing is expected to be a general feature for quadruply bonded complexes with unsaturated ligands.

Introduction

Transition-metal−alkynyl complexes are currently the subjects of considerable attention as building blocks for molecular materials.[1] In this vein, we have synthesized and studied alkynyl-substituted, quadruply metal−metal bonded complexes of the type $M_2(C{\equiv}CR)_4(PMe_3)_4$ (M = Mo, W; R = H, Me, Pr^i, Bu^t, $SiMe_3$, Ph).[2−6] These complexes can be viewed as transition-metal analogues of Diederich's tetraalkynylethenes,[7] with the central C=C unit of the latter being replaced by the M^{4}—M fragment. The electronic properties of the M_2 units can be tuned by varying the metal, the oxidation state, and the ancillary ligands,[8] thus offering a level of control over the structures and properties of materials synthesized from such building blocks that is not easily accessible to their organic counterparts.

In our prior work on $M_2(C{\equiv}CR)_4(PMe_3)_4$ complexes, we established the presence of interactions among the π/π^* levels of the alkynyl ligands and the δ/δ^* levels of the dimetal core—referred to as $\pi(C{\equiv}C)-\delta(M^{4}M)-\pi(C{\equiv}C)$ conjugation—through a variety of spectroscopic observations. These lines of evidence include the strong red shifts of the $^1(\delta{\rightarrow}\delta^*)$ transitions of $M_2(C{\equiv}CR)_4(PMe_3)_4$ complexes relative to those of $M_2X_4(PMe_3)_4$ derivatives in which M−X π-interactions are absent or weak (X = Me, halide);[2−4] the large, progressive decrease in C≡C stretching frequency with increasing electron occupancy of the δ and δ^* orbitals, reflecting M → CCR π-back-bonding;[6] and the long-range (five- and six-bond) nuclear spin−spin coupling between terminal hydrogen atoms of the alkynyl ligands and the phosphorus nuclei.[3] We have also observed that, at low temperature, the $^1(\delta{\rightarrow}\delta^*)$ absorption bands of these

[†] University of Pittsburgh.
[‡] Wabash College.
[§] Applied Detector Corporation, 1245 W. Chandler Ave., Fresno, CA 93706.

(1) Manna, J.; John, K. D.; Hopkins, M. D. *Adv. Organomet. Chem.* **1995**, *38*, 79−154.
(2) Stoner, T. C.; Dallinger, R. F.; Hopkins, M. D. *J. Am. Chem. Soc.* **1990**, *112*, 5651−5653.
(3) Stoner, T. C.; Geib, S. J.; Hopkins, M. D. *J. Am. Chem. Soc.* **1992**, *114*, 4201−4204.
(4) Stoner, T. C.; Geib, S. J.; Hopkins, M. D. *Angew. Chem., Int. Ed. Engl.* **1993**, *32*, 409−411.
(5) Stoner, T. C.; Schaefer, W. P.; Marsh, R. E.; Hopkins, M. D. *J. Cluster Sci.* **1994**, *5*, 107−124.
(6) John, K. D.; Stoner, T. C.; Hopkins, M. D. *Organometallics* **1997**, *16*, 4948−4950.
(7) Diederich, F. In *Modern Acetylene Chemistry*; Stang, P. J., and Diederich, F., Eds.; VCH: New York, 1995; pp 443−471.
(8) Cotton, F. A.; Walton, R. A. *Multiple Bonds between Metal Atoms*, 2nd ed.; Clarendon: Oxford, 1993.

10.1021/ic980866u CCC: $15.00
Published on Web 12/04/1998

complexes exhibit pronounced vibronic structure involving the nominal $\nu(M_2)$ and $\nu(MC)$ modes[2,4] and, in some cases, the $\nu(C{\equiv}C)$ mode,[6] which indicates that the molecules distort structurally along these coordinates in the $^1(\delta\delta^*)$ excited state. Such distortions could arise because the δ and/or δ^* orbitals are delocalized over the alkynyl π/π^* system, consistent with the other spectroscopic evidence for $\pi-\delta-\pi$ conjugation.[2-4,6] Alternatively, or in addition, structural distortions along the M−C and/or C≡C coordinates could result if the metal−metal stretching mode (along which the principal distortion occurs in the $^1(\delta\delta^*)$ excited state)[9] is mixed with the M−C and/or C≡C stretching modes. To distinguish between these possibilities, the interactions among the modes involving these coordinates must be understood in detail.

In this report we describe the nature of the vibrational modes of $M_2(C{\equiv}CR)_4(PMe_3)_4$ complexes, as deduced through resonance-Raman ($^1(\delta\rightarrow\delta^*)$ excitation) and nonresonance-Raman (FT-Raman) spectroscopic studies of these complexes and their selectively isotopically labeled derivatives. These studies are supported by X-ray crystallographic studies, which establish the metrical parameters of relevance to the interpretation of vibrational frequencies, and normal-coordinate calculations, which provide estimates of the contributions of various internal coordinates to the modes that give rise to the Raman bands.

Experimental Section

General Procedures. All manipulations were performed under inert atmosphere or vacuum using standard glovebox, vacuum-line, and Schlenk techniques. Solvents were distilled immediately prior to use: diethyl ether was distilled from sodium/benzophenone ketyl, tetrahydrofuran (THF) was distilled from potassium/benzophenone ketyl, toluene was distilled from sodium, 1,2-dimethoxyethane (DME) was distilled from potassium, and acetonitrile and pentane were distilled from CaH_2. Benzene-d_6 was stirred over 1:3 Na/K alloy, from which it was distilled under vacuum. Celite and molecular sieves (4 Å) were dried by heating at 80 °C under vacuum for 24 h. The compounds $Mo_2X_4(PMe_3)_4$ (X = Cl,[5] Br,[10] I[10]), $Mo_2(C{\equiv}CH)_4(PMe_3)_4$,[4] $Mo_2(C{\equiv}CSiMe_3)_4(PMe_3)_4$,[5] $Mo_2(C{\equiv}CMe)_4(PMe_3)_4$,[5] $W_2(C{\equiv}CMe)_4(PMe_3)_4$,[5] $Mo_2(C{\equiv}CBu^t)_4(PMe_3)_4$,[5] $H^{13}C{\equiv}{}^{13}CSiMe_3$,[11] $HC{\equiv}C(SiMe_3\text{-}d_9)$,[12] and $PMe_3\text{-}d_9$[13] were prepared according to standard procedures. The compounds $Mo_2X_4(PMe_3\text{-}d_9)_4$ (X = Cl, Br, I, C≡CH, $C{\equiv}CSiMe_3$), $Mo_2(^{13}C{\equiv}{}^{13}CSiMe_3)_4(PMe_3)_4$, and $Mo_2(C{\equiv}CSiMe_3\text{-}d_9)_4(PMe_3)_4$ were prepared via the procedures for their natural-abundance isotopomers using appropriate labeled reagents. All other chemicals were used as received.

Spectroscopic Measurements. NMR spectra were recorded with a Bruker AF500 NMR spectrometer. Infrared spectra of neat films (evaporated from solution), mineral oil mulls, or solutions, contained in an airtight sodium chloride cell, were measured with an IBM IR-32 spectrometer at 2.0 cm^{-1} resolution.

Resonance-Raman spectra of THF solutions in 5 mm NMR tubes were obtained using 632.8 nm excitation from a He−Ne laser. Samples were spun at ~40 Hz to minimize local heating effects. Nonlasing emission lines were eliminated with a narrow band-pass filter (632.8 nm, 3 nm fwhm). The laser power at the sample was ca. 7 mW. Backscattered Raman radiation was dispersed with a 0.85 m double monochromator; the spectral band-pass of the monochromator was 4.0 cm^{-1}. The Raman signal was detected by a cooled Hamamatzu R928 photomultiplier tube and processed by a photon-counting system.

FT-Raman spectra of crystalline solids in capillary tubes were recorded using a Nicolet 950 spectrometer (Nd:YVO_4 source, $\lambda = 1064$ nm) at 1 cm^{-1} resolution. The notch filter in this instrument requires the application of a large background correction (KBr standard) for $\Delta\nu < 130$ cm^{-1}; thus, relative intensities are irreproducible in this region. Peak positions are reproducible to ±1 cm^{-1} for $\Delta\nu \geq 100$ cm^{-1}. The Raman signal was detected with an Applied Detector Corp. high-purity germanium-diode detector (model 203NR). Data reduction was accomplished using Nicolet Omnic software (version 1.1). Frequencies were calibrated using acetonitrile as an external reference.

$[NBu^n_4]F{\cdot}x(D_2O)$. Tetrabutylammonium fluoride hydrate (10.60 g, 33.5 mmol for $x = 0$) was dissolved in 30 mL of D_2O. The solution was stirred for 4 h and the solvent then removed in vacuo at 25 °C. This process was repeated four times. The gelatinous product was then dissolved in 50 mL of DME and transferred by cannula to a flask containing molecular sieves (4 Å). The solution was stirred for 24 h and filtered through Celite prior to use.

$Mo_2(C{\equiv}CD)_4(PMe_3)_4$. This compound was prepared by a variation of the reported procedure for the natural-abundance compound.[4] A solution of $[NBu^n_4]F{\cdot}x(D_2O)$, prepared as above, was added to a stirred, room-temperature suspension of $Mo_2(C{\equiv}CSiMe_3)_4(PMe_3)_4$ (7.45 g, 8.42 mmol) in DME (50 mL). The reaction mixture was warmed to 45 °C and monitored periodically by electronic-absorption spectroscopy ($Mo_2(C{\equiv}CSiMe_3)_4(PMe_3)_4$, $\lambda_{max} = 692$ nm; $Mo_2(C{\equiv}CD)_4(PMe_3)_4$, $\lambda_{max} = 660$ nm). The initial royal-blue color of the reaction mixture darkened slightly as the reaction proceeded. When the reaction was complete (ca. 1 h), the volatile components were removed in vacuo at 45 °C. The remaining solid was extracted with pentane (30 mL) and the solution filtered through Celite. Removal of the solvent under vacuum yielded the blue crude product; this was dissolved in a minimum amount of diethyl ether (5 mL), which was then layered with acetonitrile (5 mL) and allowed to stand undisturbed at −40 °C for 12 h, at which time 1.90 g of dark-blue crystals (3.16 mmol, 38% yield) was isolated by filtration. On the basis of the ratio of the integrated intensity of the C*CH* resonance to that of the P*Me*$_3$ resonance in the ^{1}H-NMR spectrum of the product, the extent of deuterium labeling of the ethynyl ligands is 86 atom %.

^{1}H NMR (300.13 MHz, C_6D_6, 25 °C): δ 4.38 (pseudo quin, 0.56 H, C*CH*); 1.71 (virtual t, 36 H, P*Me*$_3$). IR (Neat film): 1912 cm^{-1} (vw), ν(C≡CH); 1806 cm^{-1} (w), ν(C≡CD).

Single-Crystal X-ray Diffraction Studies. Single-crystal X-ray diffraction experiments were performed on a Siemens R3 diffractometer with graphite-monochromated Mo Kα ($\lambda = 0.710\,73$ Å) radiation. Diffraction data were refined using the Siemens SHELXTL PLUS (version 5.02) software package on a Silicon Graphics Indigo system.

Single crystals of $Mo_2(C{\equiv}CMe)_4(PMe_3)_4$, $W_2(C{\equiv}CMe)_4(PMe_3)_4$, and $Mo_2(C{\equiv}CBu^t)_4(PMe_3)_4$ suitable for X-ray diffraction were obtained by layering concentrated diethyl ether solutions of these complexes with acetonitrile and cooling to −25 °C. Single crystals of $Mo_2(C{\equiv}CSiMe_3)_4(PMe_3)_4$ were obtained via slow evaporation of a toluene solution of the complex. Crystals were coated in Fluorolube and mounted on a glass fiber at −65 °C.

Lattice parameters were determined from a least-squares fit of the angular settings of 24 reflections in the range $20° \leq 2\theta \leq 25°$. The intensities of three representative reflections were measured every 197 reflections to check for decay of the crystal. The molybdenum complexes showed no signs of decay through the course of the data collection, but a ca. 10% loss of intensity was observed for $W_2(C{\equiv}CMe)_4(PMe_3)_4$ (crystals of which are thermally unstable and especially air sensitive); a correction for the decay was applied to the data. An empirical absorption correction (XEMP), based on azimuthal scans of six reflections, was performed. All data were corrected for Lorentz and polarization effects. The crystal data and refinement parameters are set out in Table 1.

The metal and phosphorus atoms were located using direct methods; remaining atoms were located from subsequent difference-Fourier syntheses and refined anistropically, except for $Mo_2(C{\equiv}CBu^t)_4(PMe_3)_4$ (vide infra). Hydrogen-atom positions were computed by fixing the

(9) Cotton, F. A.; Walton, R. A. *Multiple Bonds between Metal Atoms*, 2nd ed.; Clarendon: Oxford, 1993; pp 687−719.
(10) Hopkins, M. D.; Schaefer, W. P.; Bronikowski, M. J.; Woodruff, W. H.; Miskowski, V. M.; Dallinger, R. F.; Gray, H. B. *J. Am. Chem. Soc.* **1987**, *109*, 408−416.
(11) $H^{13}C{\equiv}{}^{13}CSiMe_3$ was prepared according to the procedure for $H^{13}C{\equiv}{}^{13}CSiEt_3$ (Kamieñska-Trela, K.; Lüttke, W. *Pol. J. Chem.* **1980**, *54*, 611−615) and extracted and purified using standard procedures for alkynes (ref 12).
(12) Brandsma, L. *Preparative Acetylenic Chemistry*, 2nd ed.; Elsevier: New York, 1988; p 5.
(13) Bergman, R. G.; Wenzel, T. T. *J. Am. Chem. Soc.* **1986**, *108*, 4856−4857.

Table 1. Crystallographic Data for $Mo_2(C{\equiv}CR)_4(PMe_3)_4$ Complexes

parameter	$Mo_2(C{\equiv}CMe)_4(PMe_3)_4$	$W_2(C{\equiv}CMe)_4(PMe_3)_4$	$Mo_2(C{\equiv}CSiMe_3)_4(PMe_3)_4$	$Mo_2(C{\equiv}CBu^t)_4(PMe_3)_4$
empirical formula	$C_{24}H_{48}Mo_2P_4$	$C_{24}H_{48}P_4W_2$	$C_{32}H_{72}Mo_2P_4Si_4$	$C_{36}H_{72}Mo_2P_4$
fw	652.38	828.20	885.02	820.72
space group	$P\bar{1}$ (No. 2)	$P\bar{1}$ (No. 2)	*Pnma* (No. 62)	$Pna2_1$ (No. 33)
a, Å	11.673(2)	11.682(2)	19.550(5)	13.498(3)
b, Å	16.317(3)	16.294(4)	18.346(5)	18.056(5)
c, Å	18.568(4)	18.674(5)	14.473(3)	19.805(4)
α, deg	108.98(3)	109.61(2)	90	90
β, deg	92.28(3)	92.43(2)	90	90
γ, deg	91.07(3)	91.10(2)	90	90
V, Å^3	3339.8(11)	3343.2(13)	5191(2)	4827(2)
ρ_{calcd}, g cm^{-3}	1.297	1.645	1.132	1.129
Z	4	4	4	4
μ, cm^{-1}	9.52	70.76	7.16	6.71
λ(Mo Kα), Å	0.710 73	0.710 73	0.710 73	0.710 73
T, °C	−65	−65	−65	−65
R1 [$I > 2\sigma(I)$], %[a]	2.92	4.09	4.44	7.54
wR2 [$I > 2\sigma(I)$], %[b]	6.60	8.32	9.13	17.56
R1 (all data), %[a]	4.10	7.45	7.74	11.07
wR2 (all data), %[b]	7.22	10.12	11.87	19.81

[a] $R1 = \sum||F_o| - |F_c||/\sum|F_o|$. [b] $wR2 = [\sum[w(F_o^2 - F_c^2)^2]/\sum[w(F_o^2)^2]]^{1/2}$.

C−H distance to 0.96 Å and by assuming a staggered configuration. The structures of $Mo_2(C{\equiv}CMe)_4(PMe_3)_4$ and $W_2(C{\equiv}CMe)_4(PMe_3)_4$ were solved straightforwardly.

$Mo_2(C{\equiv}CSiMe_3)_4(PMe_3)_4$. Refinement revealed an apparently ordered set of alkynyl and phosphine ligands within which the Mo_2 unit is disordered among three pairs of sites with roughly orthogonal orientations. Two Mo_2 orientations are related by mirror symmetry. The metal-atom disorder was modeled by refining the dimolybdenum units with a shared free variable that assigned the occupation of the sites on the basis of the observed electron density. The site-occupancy factors (SOFs) of Mo(1) and Mo(2) (the principal pair) were allowed to vary against the sum of Mo(1′) and Mo(2′); these factors were constrained such that the total Mo_2 occupancy was unity. Modeling in this fashion resulted in site-occupancy factors of 0.796, 0.102, and 0.102 for the three orientations. Analysis of the difference map failed to reveal candidates for disordered ligand sites associated with the minor-occupancy Mo_2 units.

$Mo_2(C{\equiv}CBu^t)_4(PMe_3)_4$. Crystals of $Mo_2(C{\equiv}CBu^t)_4(PMe_3)_4$ were shown to adopt the chiral space group $Pna2_1$. The absolute configuration was established by refinement of the Flack parameter.[14] The crystals diffracted poorly, and there were insufficient data to allow anisotropic refinement of the carbon atoms; these were refined isotropically. Refinement revealed a disordered Mo_2 core with three roughly orthogonal orientations within an apparently ordered set of ligands. In the initial stages of the refinement the SOFs of the minor pairs, Mo(1′)/Mo(2′) and Mo(1″)/Mo(2″), were constrained to be equal to each other and the SOFs of Mo(1) and Mo(2) (the principal pair) were allowed to vary against the sum of Mo(1′)/Mo(2′) and Mo(1″)/Mo(2″); this gave SOFs of 0.648, 0.176, and 0.176. The SOF of Mo(1)/Mo(2) was then fixed to 0.648, and the SOFs of Mo(1′)/Mo(2′) and Mo(1″)/ Mo(2″) were allowed to refine freely against each other, giving values of 0.211 and 0.141, respectively. The final refinement gave SOFs of 0.648 (Mo(1)/Mo(2)), 0.211 (Mo(1′)/Mo(2′)), and 0.141 (Mo(1″)/Mo(2″)) for the three orientations. One of the alkynyl Bu^t groups is rotationally disordered such that there are two orientations that are 60° out of phase. Modeling for the two orientations of the methyl carbon atoms gave site-occupancy factors of 0.563 and 0.437.

Normal-Coordinate Calculations. Normal-coordinate calculations employed the Schachtschneider formulation.[15,16] Geometries for $Mo_2Cl_4P_4$ and $Mo_2(C{\equiv}CH)_4P_4$, where the PMe_3 ligand is approximated as a phosphorus atom, were taken from X-ray crystal structures of $Mo_2Cl_4(PMe_3)_4$[17] and $Mo_2(C{\equiv}CH)_4(PMe_3)_4$,[4] respectively. Chemically equivalent bond distances and angles were averaged to D_{2d} symmetry; for $Mo_2(C{\equiv}CH)_4P_4$, the nonlinearity of the MoC≡CH unit (∠(Mo−C≡C) = 171.8[4]°, ∠(C≡C−H) = 169.4[24]°) was included in such a way as to preserve D_{2d} symmetry. Couplings between oscillators located on different metal centers were neglected in all calculations. Valence force constants are represented by the symbol *f*.

Because there are many more variables in these calculations than there are observed frequencies, the calculations were conducted in discrete stages. Initially, stretching and stretch−stretch force constants were calculated by fitting only those stretching modes with experimentally well established frequencies. As additional force constants were introduced, the previously optimized ones were initially fixed, and the new and old sets of force constants were optimized in alternating cycles. This procedure was particularly crucial in the final stages of refinement where the fit was to a largely unassigned group of low-frequency bands.

For $Mo_2Cl_4P_4$, the four highest-frequency core modes of $Mo_2Cl_4(PMe_3)_4$ (ν_1 [a_1, $\nu(Mo_2)$], ν_2 [a_1, ν(MoCl)], ν_6 [b_2, ν(MoCl)], and ν_{10} [e, ν(MoCl)]) were fitted first with two stretching force constants ($f(Mo_2)$ and f(MoCl)) and two stretch−stretch interaction force constants ($f(Mo_2,MoCl)$ and (f(MoCl,MoCl)). A sizable value for $f(Mo_2,MoCl)$ (ca. +0.3 mdyn Å^{-1}) was required to reproduce the large splittings observed among ν_2 [a_1, ν(MoCl)], ν_6 [b_2, ν(MoCl)], and ν_{10} [e, ν(MoCl)]. M−P stretching and metal−ligand bending force constants were subsequently added to the force field, with f(MoP), f(MoMoCl), and f(MoMoP) initially assumed to have values of 1.0 mdyn Å^{-1}, 1.0 mdyn Å rad^{-2}, and 0.5 mdyn Å rad^{-2}, and $f(Mo_2,MoP)$ and f(MoP, MoP) assigned values of 0.1 mdyn Å^{-1}; all bands observed in the present study and from prior reports[10,18−20] (other than internal PMe_3 modes) were included in the fit. Finally, one additional stretch−stretch interaction force constant (f(MoCl,MoP)) and four stretch−bend interaction force constants ($f(Mo_2,MoMoCl)$, $f(Mo_2,MoMoP)$, f(MoCl, MoMoCl), f(MoP,MoMoP)), initially assumed to have values of 0.1 mdyn Å^{-1} and 0.1 mdyn rad^{-1}, respectively, were added to the force field.

In trial calculations we either neglected metal−metal torsion or included a torsion force constant (f_τ) ranging from 0.083 mdyn Å rad^{-2} (a value suggested by a molecular-mechanics calculation)[21] to 0.5 mdyn

(14) Flack, H. D. *Acta Crystallogr.* **1983**, *A39*, 876−881.
(15) Schachtschneider, J. H. Reports 231/64 and 57/65; Shell Development Company: Houston, TX.
(16) McIntosh, D. F.; Peterson, M. R. *General Vibrational Analysis Programs Utilizing the Wilson GF Matrix Method for a General Unsymmetrical Molecule*; Program No. 342, Quantum Chemistry Program Exchange, Department of Chemistry, Indiana University, Bloomington, IN (Internet address file://qcpe6.chem.indiana.edu/).
(17) Cotton, F. A.; Extine, M. W.; Felthouse, T. R.; Kolthammer, B. W. S.; Lay, D. G. *J. Am. Chem. Soc.* **1981**, *103*, 4040−4045.
(18) Svendsen, C.; Nielsen, M. J.; Mortensen, O. S.; Allers, S. J. R.; Clark, R. J. H. *Chem. Phys.* **1997**, *215*, 89−96.
(19) Carlin, R. T.; McCarley, R. E. *Inorg. Chem.* **1989**, *28*, 280−282.
(20) Hopkins, M. D.; Miskowski, V. M.; Killough, P. M.; Sattelberger, A. P.; Woodruff, W. H.; Gray, H. B. *Inorg. Chem.* **1992**, *31*, 5368−5374.

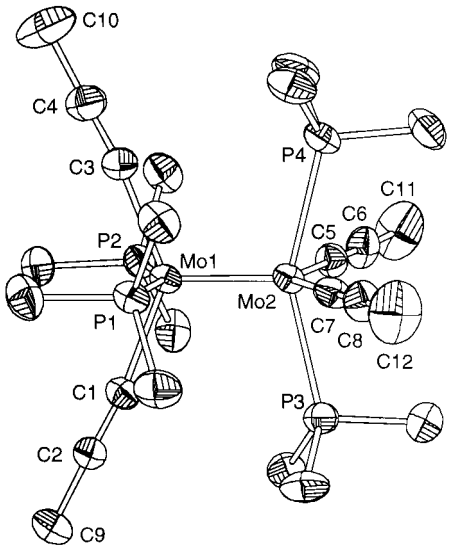

Figure 1. Thermal-ellipsoid representation of $Mo_2(C{\equiv}CMe)_4(PMe_3)_4$, drawn at the 40% probability level. Only one of the two molecules in the asymmetric unit is shown. Hydrogen atoms have been omitted for clarity.

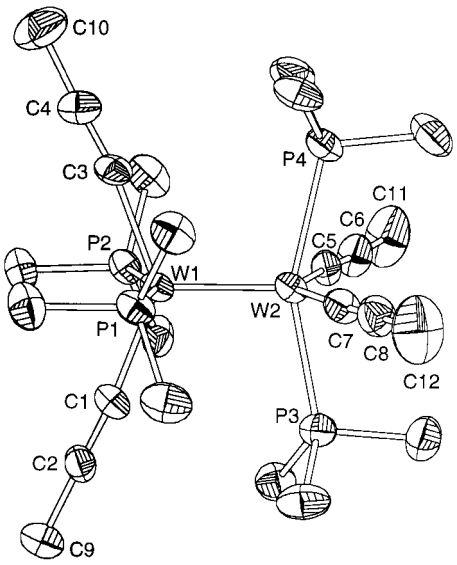

Figure 2. Thermal-ellipsoid representation of $W_2(C{\equiv}CMe)_4(PMe_3)_4$, drawn at the 40% probability level. Only one of the two molecules in the asymmetric unit is shown. Hydrogen atoms have been omitted for clarity.

Å rad^{-2}. Regardless of the assumed value of f_τ, the torsional mode (always the lowest-frequency nonzero eigenvalue) was calculated to be >95% pure; thus, this mode is excluded from the reported results because it has no effect upon observable frequencies.

For $Mo_2(C{\equiv}CH)_4P_4$, common force constants were imported from the $Mo_2Cl_4P_4$ force field and f(MoC) (2.000 mdyn $Å^{-1}$), f(MoCC) (0.260 mdyn Å rad^{-2}), and f(C≡C,MoC) (0.200 mdyn $Å^{-1}$) were estimated from force fields for metal−cyanide complexes;[22−24] these force constants were fixed. Initial values for internal force constants of the CCH unit were taken from force fields for $CH_3C{\equiv}CH$[25] and XC≡CH (X = Cl, Br, I);[26] these were refined in the calculations to fit the observed ν(≡CH) and ν(C≡C) modes of $Mo_2(C{\equiv}CH)_4(PMe_3)_4$, $Mo_2(C{\equiv}CH)_4(PMe_3\text{-}d_9)_4$, and $Mo_2(C{\equiv}CD)_4(PMe_3)_4$. (We did not attempt to reproduce the observed splitting of ν(≡CH) (vide infra) in the calculations but, instead, averaged these frequencies.) It was evident at this point that calculated frequencies and potential-energy distributions (PEDs) of the core modes were in qualitative agreement with the FT-Raman and resonance-Raman data for $Mo_2(C{\equiv}CH)_4(PMe_3)_4$ and $Mo_2(C{\equiv}CSiMe_3)_4(PMe_3)_4$, respectively. Due to the enormously underdetermined nature of the problem—there are 24 force constants in this treatment (if metal−metal torsion is included) and 36 calculated modes, 12 of which are degenerate—we viewed more extensive force constant variation as an unrealistic and unproductive exercise.

Results and Discussion

Single-Crystal X-ray Diffraction Studies. The molecular structures of the complexes $Mo_2(C{\equiv}CMe)_4(PMe_3)_4$, $Mo_2(C{\equiv}CBu^t)_4(PMe_3)_4$, $Mo_2(C{\equiv}CSiMe_3)_4(PMe_3)_4$, and $W_2(C{\equiv}CMe)_4(PMe_3)_4$ were determined through single-crystal X-ray diffraction studies. Thermal-ellipsoid representations of the structures of these complexes are shown in Figures 1−4, and selected bond distances and bond angles are set out in Tables 2−5.

The crystal structures of the (isomorphous) $M_2(C{\equiv}CMe)_4(PMe_3)_4$ complexes (Figures 1 and 2) are ordered, but those of $Mo_2(C{\equiv}CSiMe_3)_4(PMe_3)_4$ (Figure 3) and $Mo_2(C{\equiv}CBu^t)_4(PMe_3)_4$ (Figure 4) exhibit disorder of the Mo_2 units along three roughly orthogonal axes that are normal to the faces of the approximate cube formed by the coordinating atoms of the ligands. Disorder of this type[27] has been observed for other $M_2X_4(PR_3)_4$ complexes for which the size of the PR_3 ligand significantly exceeds that of X, such as for $Mo_2F_4(PMe_3)_4$,[28]

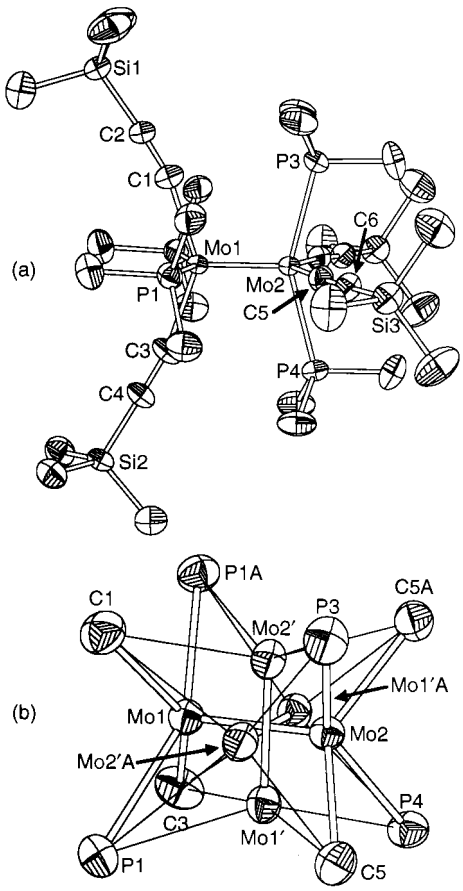

Figure 3. Thermal-ellipsoid representation of the molecular structure of $Mo_2(C{\equiv}CSiMe_3)_4(PMe_3)_4$, drawn at the 30% probability level: (a) major-occupancy dimer; (b) disordered core. Hydrogen atoms have been omitted for clarity.

(21) Boeyens, J. C. A.; O'Neil, F. M. M. *Inorg. Chem.* **1995**, *34*, 1988−1995.
(22) Jones, L. H. *Inorg. Chem.* **1965**, *4*, 1472−1475.
(23) Jones, L. H. *J. Chem. Phys.* **1957**, *27*, 468−472.
(24) Jones, L. H. *J. Chem. Phys.* **1957**, *26*, 1578−1584.
(25) Daykin, P. N.; Sundaram, S.; Cleveland, F. F. *J. Chem. Phys.* **1962**, *37*, 1087−1094.
(26) Lichene, F.; Dellepiane, G.; Lorenzelli, V. *J. Chem. Phys.* **1979**, *70*, 4786−4796.

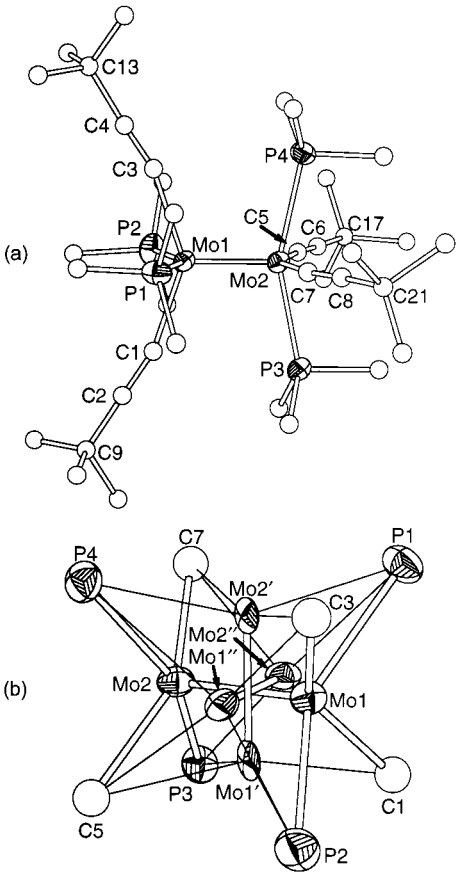

Figure 4. Thermal-ellipsoid representation of the molecular structure of $Mo_2(C{\equiv}CBu^t)_4(PMe_3)_4$, drawn at the 30% probability level: (a) major-occupancy dimer; (b) disordered core. Hydrogen atoms have been omitted for clarity.

$M_2Cl_4(PEt_3)_4$ (M = Mo,[29] Tc,[30] Re[29]), $W_2Cl_4(PBu^n_3)_4$,[31] and $Re_2X_4(PPr^n_3)_4$ (X = Cl, Br),[31] or vice versa, as for $Mo_2(C{\equiv}CPr^i)_4(PMe_3)_4$,[5] with the occupancies of the disordered M_2 sites either being equal (1/3)[28−30] or different for all three orientations.[5,31] The structure of $Mo_2(C{\equiv}CBu^t)_4(PMe_3)_4$ is of the latter type; the site-occupancy factors (SOFs) for the Mo_2 unit are 0.648, 0.211, and 0.141. The disorder observed for $Mo_2(C{\equiv}CSiMe_3)_4(PMe_3)_4$ is of a type not previously observed for $M_2X_4(PR_3)_4$ complexes in that two of the orientations are related through crystallographic symmetry (in this case, mirror symmetry); the SOFs are 0.796, 0.102, and 0.102. Careful analysis of the difference map failed to reveal candidates for disordered ligand sites associated with the minor-occupancy Mo_2 units. As a result, the Mo−P and Mo−C bond distances of the minor-occupancy dimers span chemically unrealistically wide ranges. It is noteworthy, however, that the most anomalous Mo−P distance for the minor-occupancy dimer (d(Mo(1′)−P(4)) = 2.384(4) Å, Table 4) is coupled with an anomalously long distance for the major-occupancy dimer (d(Mo(2)−P(4)) = 2.523(2) Å), which is outside the range of distances for the ordered structures of $Mo_2(C{\equiv}CMe)_4(PMe_3)_4$ (2.5009(11)−2.5133(13) Å, Table 2) and $Mo_2(C{\equiv}CH)_4(PMe_3)_4$ (2.509(1)−2.515(1) Å).[4] This suggests that the refined ligand-atom positions are averages over disordered positions that differ vectorially by as much as ∼0.15 Å (P(4)) or ∼0.30 Å (alkynyl carbon atom C(1)). As Parkin has noted,[32] this is not an unusual situation given the intrinsic resolution limits of X-rays.

Table 2. Selected Bond Distances (Å) and Angles (deg) for $Mo_2(C{\equiv}CMe)_4(PMe_3)_4$

molecule 1		molecule 2	
	Distances (Å)		
Mo(1)−Mo(2)	2.1414(9)	Mo(1′)−Mo(2′)	2.1398(7)
Mo(1)−C(1)	2.147(3)	Mo(1′)−C(1′)	2.147(4)
Mo(1)−C(3)	2.147(4)	Mo(1′)−C(3′)	2.140(4)
Mo(2)−C(5)	2.141(4)	Mo(2′)−C(5′)	2.146(4)
Mo(2)−C(7)	2.140(3)	Mo(2′)−C(7′)	2.146(4)
Mo(1)−P(1)	2.5091(11)	Mo(1′)−P(1′)	2.5133(13)
Mo(1)−P(2)	2.5081(10)	Mo(1′)−P(2′)	2.5070(13)
Mo(2)−P(3)	2.5088(11)	Mo(2′)−P(3′)	2.5086(12)
Mo(2)−P(4)	2.5085(10)	Mo(2′)−P(4′)	2.5009(11)
C(1)−C(2)	1.203(4)	C(1′)−C(2′)	1.198(5)
C(2)−C(9)	1.475(5)	C(2′)−C(9′)	1.479(5)
C(3)−C(4)	1.195(5)	C(3′)−C(4′)	1.184(5)
C(4)−C(10)	1.470(6)	C(4′)−C(10′)	1.477(6)
C(5)−C(6)	1.199(5)	C(5′)−C(6′)	1.200(5)
C(6)−C(11)	1.474(6)	C(6′)−C(11′)	1.476(5)
C(7)−C(8)	1.196(5)	C(7′)−C(8′)	1.198(5)
C(8)−C(12)	1.477(5)	C(8′)−C(12′)	1.473(5)
	Angles (deg)		
Mo(2)−Mo(1)−C(1)	110.74(9)	Mo(2′)−Mo(1′)−C(1′)	110.38(10)
Mo(2)−Mo(1)−C(3)	111.41(10)	Mo(2′)−Mo(1′)−C(3′)	112.41(10)
Mo(1)−Mo(2)−C(5)	110.99(9)	Mo(1′)−Mo(2′)−C(5′)	111.16(9)
Mo(1)−Mo(2)−C(7)	109.95(10)	Mo(1′)−Mo(2′)−C(7′)	110.16(10)
Mo(1)−Mo(2)−P(3)	102.78(3)	Mo(1′)−Mo(2′)−P(3′)	102.75(3)
Mo(1)−Mo(2)−P(4)	103.48(4)	Mo(1′)−Mo(2′)−P(4′)	102.68(4)
Mo(2)−Mo(1)−P(1)	102.62(4)	Mo(2′)−Mo(1′)−P(1′)	102.30(4)
Mo(2)−Mo(1)−P(2)	101.38(4)	Mo(2′)−Mo(1′)−P(2′)	101.64(3)
P(2)−Mo(1)−P(1)	156.00(3)	P(2′)−Mo(1′)−P(1′)	155.95(4)
P(4)−Mo(2)−P(3)	153.74(4)	P(4′)−Mo(2′)−P(3′)	154.57(4)
C(1)−Mo(1)−C(3)	137.81(13)	C(1′)−Mo(1′)−C(3′)	137.21(14)
C(7)−Mo(2)−C(5)	139.02(13)	C(5′)−Mo(2′)−C(7′)	138.65(14)
C(2)−C(1)−Mo(1)	172.1(3)	C(2′)−C(1′)−Mo(1′)	174.5(3)
C(4)−C(3)−Mo(1)	172.1(3)	C(4′)−C(3′)−Mo(1′)	167.3(3)
C(6)−C(5)−Mo(2)	172.2(3)	C(6′)−C(5′)−Mo(2′)	171.4(3)
C(8)−C(7)−Mo(2)	175.8(3)	C(8′)−C(7′)−Mo(2′)	173.0(3)
C(1)−C(2)−C(9)	177.5(4)	C(1′)−C(2′)−C(9′)	177.9(4)
C(3)−C(4)−C(10)	177.9(4)	C(3′)−C(4′)−C(10′)	178.3(5)
C(5)−C(6)−C(11)	178.8(4)	C(5′)−C(6′)−C(11′)	176.5(4)
C(7)−C(8)−C(12)	176.9(5)	C(7′)−C(8′)−C(12′)	177.9(4)

The molecular structures of all four complexes conform closely to the idealized D_{2d} symmetry typically found for $M_2X_4(PMe_3)_4$ complexes, although the crystallographically imposed symmetries are C_1 ($Mo_2(C{\equiv}CMe)_4(PMe_3)_4$ and $Mo_2(C{\equiv}CBu^t)_4(PMe_3)_4$) or C_s ($Mo_2(C{\equiv}CSiMe_3)_4(PMe_3)_4$). The two $M(C{\equiv}CR)_2(PMe_3)_2$ units in each dimer exhibit average C−M−M−P torsion angles of <2° ($M_2(C{\equiv}CMe)_4(PMe_3)_4$ (M = Mo, W), 1.5°; $Mo_2(C{\equiv}CSiMe_3)_4(PMe_3)_4$, 1.3°; $Mo_2(C{\equiv}CBu^t)_4(PMe_3)_4$, 0.6°). Among the $Mo_2(C{\equiv}CR)_4(PMe_3)_4$ compounds, the M−M and M−P distances and M−M−P angles are similar to those reported previously for the parent complex $Mo_2(C{\equiv}CH)_4(PMe_3)_4$[4] and are well within the ranges established for halide and pseudo-halide $Mo_2X_4(PMe_3)_4$ derivatives,[10,17,28,33−35] while the corresponding distances and angles for $W_2(C{\equiv}CMe)_4(PMe_3)_4$ are close to those for 1,1,2′,2′-$W_2(C{\equiv}CMe)_2Cl_2(PMe_3)_4$[3] and $W_2Cl_4(PMe_3)_4$;[17] these comparisons are set out in Table 6. The W−W distance of $W_2(C{\equiv}CMe)_4(PMe_3)_4$ is 0.136 Å longer than that of the molybdenum analogue; this difference is essentially the same as that between the related $M_2Cl_4(PMe_3)_4$ complexes[17] of these metals (0.132 Å). Interestingly, the W−W bond length of 1,1,2′,2′-$W_2(C{\equiv}CMe)_2Cl_2$-

(27) Cotton, F. A.; Walton, R. A. *Multiple Bonds between Metal Atoms*, 2nd ed.; Clarendon: Oxford, 1993; pp 641−645.
(28) Cotton, F. A.; Wiesinger, K. J. *Inorg. Chem.* **1992**, *31*, 920−925.
(29) Cotton, F. A.; Daniels, L. M.; Shang, M.; Yao, Z. *Inorg. Chim. Acta* **1994**, *215*, 103−107.
(30) Burns, C. J.; Burrell, A. K.; Cotton, F. A.; Haefner, S. C.; Sattelberger, A. P. *Inorg. Chem.* **1994**, *33*, 2257−2264.
(31) Cotton, F. A.; Jennings, J. G.; Price, A. C.; Vidyasagar, K. *Inorg. Chem.* **1990**, *29*, 4138−4143.
(32) Parkin, G. *Chem. Rev.* **1993**, *93*, 887−911.

Table 3. Selected Bond Distances (Å) and Angles (deg) for $W_2(C{\equiv}CMe)_4(PMe_3)_4$

molecule 1		molecule 2	
	Distances (Å)		
W(1)−W(2)	2.2742(9)	W(1′)−W(2′)	2.2777(7)
W(1)−C(1)	2.103(9)	W(1′)−C(3′)	2.126(10)
W(1)−C(3)	2.111(9)	W(1′)−C(1′)	2.129(9)
W(2)−C(5)	2.139(11)	W(2′)−C(5′)	2.135(10)
W(2)−C(7)	2.125(10)	W(2′)−C(7′)	2.129(9)
W(1)−P(1)	2.502(3)	W(1′)−P(1′)	2.494(3)
W(1)−P(2)	2.494(3)	W(1′)−P(2′)	2.484(2)
W(2)−P(3)	2.483(3)	W(2′)−P(4′)	2.480(2)
W(2)−P(4)	2.486(2)	W(2′)−P(3′)	2.496(3)
C(1)−C(2)	1.200(11)	C(1′)−C(2′)	1.176(12)
C(2)−C(9)	1.489(12)	C(2′)−C(9′)	1.492(13)
C(3)−C(4)	1.202(12)	C(3′)−C(4′)	1.188(14)
C(4)−C(10)	1.482(14)	C(4′)−C(10′)	1.49(2)
C(5)−C(6)	1.208(13)	C(5′)−C(6′)	1.194(13)
C(6)−C(11)	1.471(14)	C(6′)−C(11′)	1.480(13)
C(7)−C(8)	1.203(13)	C(7′)−C(8′)	1.179(11)
C(8)−C(12)	1.48(2)	C(8′)−C(12′)	1.494(12)
	Angles (deg)		
W(2)−W(1)−C(1)	110.6(3)	W(2′)−W(1′)−C(1′)	110.4(3)
W(2)−W(1)−C(3)	110.9(2)	W(2′)−W(1′)−C(3′)	112.1(3)
W(1)−W(2)−C(5)	110.4(2)	W(1′)−W(2′)−C(5′)	111.1(2)
W(1)−W(2)−C(7)	109.4(3)	W(1′)−W(2′)−C(7′)	109.6(3)
W(1)−W(2)−P(3)	101.38(7)	W(1′)−W(2′)−P(3′)	101.54(7)
W(1)−W(2)−P(4)	102.15(7)	W(1′)−W(2′)−P(4′)	101.00(7)
W(2)−W(1)−P(1)	100.87(6)	W(2′)−W(1′)−P(1′)	101.16(7)
W(2)−W(1)−P(2)	99.92(6)	W(2′)−W(1′)−P(2′)	99.95(7)
P(2)−W(1)−P(1)	159.22(8)	P(2′)−W(1′)−P(1′)	158.77(9)
P(3)−W(2)−P(4)	156.47(9)	P(3′)−W(2′)−P(4′)	157.46(9)
C(1)−W(1)−C(3)	138.5(3)	C(1′)−W(1′)−C(3′)	137.5(4)
C(7)−W(2)−C(5)	140.2(3)	C(7′)−W(2′)−C(5′)	139.3(4)
C(2)−C(1)−W(1)	173.9(9)	C(2′)−C(1′)−W(1′)	174.9(10)
C(4)−C(3)−W(1)	171.8(8)	C(4′)−C(3′)−W(1′)	167.7(9)
C(6)−C(5)−W(2)	171.6(8)	C(6′)−C(5′)−W(2′)	170.4(9)
C(8)−C(7)−W(2)	175.6(9)	C(8′)−C(7′)−W(2′)	173.0(10)
C(1)−C(2)−C(9)	178.4(10)	C(1′)−C(2′)−C(9′)	176.5(12)
C(3)−C(4)−C(10)	177.2(11)	C(3′)−C(4′)−C(10′)	177.0(14)
C(5)−C(6)−C(11)	176.8(12)	C(5′)−C(6′)−C(11′)	177.8(11)
C(7)−C(8)−C(12)	178.0(12)	C(7′)−C(8′)−C(12′)	178.1(12)

Table 4. Selected Bond Distances (Å) and Angles (deg) for $Mo_2(C{\equiv}CSiMe_3)_4(PMe_3)_4$[a]

major-occupancy dimer		minor-occupancy dimers	
	Distances (Å)		
Mo(1)−Mo(2)	2.1355(10)	Mo(1′)−Mo(2′)	2.119(5)
Mo(1)−C(1)	2.138(7)	Mo(2′)−C(1)	2.434(8)
Mo(1)−C(3)	2.154(7)	Mo(1′)−C(3)	2.371(7)
Mo(2)−C(5)	2.162(5)	Mo(1′)−C(5)	2.220(6)
		Mo(2′)−C(5)A	2.225(6)
Mo(1)−P(1)	2.5039(14)	Mo(1′)−P(1)	2.560(4)
Mo(2)−P(3)	2.505(2)	Mo(2′)−P(3)	2.420(4)
Mo(2)−P(4)	2.523(2)	Mo(1′)−P(4)	2.384(4)
		Mo(2′)−P(1)A	2.579(4)
C(1)−C(2)	1.203(8)		
C(3)−C(4)	1.214(8)		
C(5)−C(6)	1.214(6)		
Si(1)−C(2)	1.803(7)		
Si(2)−C(4)	1.813(7)		
Si(3)−C(6)	1.814(5)		
	Angles (deg)		
Mo(2)−Mo(1)−C(1)	108.4(2)	Mo(1′)−Mo(2′)−C(1)	100.8(2)
Mo(2)−Mo(1)−C(3)	108.5(2)	Mo(2′)−Mo(1′)−C(3)	97.9(2)
Mo(1)−Mo(2)−C(5)	109.27(12)	Mo(2′)−Mo(1′)−C(5)	97.5(2)
		Mo(1′)−Mo(2′)−C(5)A	101.8(2)
Mo(1)−Mo(2)−P(3)	103.64(5)	Mo(1′)−Mo(2′)−P(3)	108.8(2)
Mo(1)−Mo(2)−P(4)	104.69(5)	Mo(2′)−Mo(1′)−P(4)	103.9(2)
Mo(2)−Mo(1)−P(1)	103.03(3)	Mo(2′)−Mo(1′)−P(1)	102.9(2)
		Mo(1′)−Mo(2′)−P(1)A	106.5(2)
C(1)−Mo(1)−C(3)	143.1(3)	C(5)A−Mo(2′)−C(1)	157.0(2)
C(5)A−Mo(2)−C(5)	141.4(2)	C(5)−Mo(1′)−C(3)	164.0(2)
P(1)A−Mo(1)−P(1)	153.94(7)	P(4)−Mo(1′)−P(1)	153.1(2)
P(3)−Mo(2)−P(4)	151.67(7)	P(3)−Mo(2′)−P(1)A	144.3(2)
C(2)−C(1)−Mo(1)	166.6(7)	C(2)−C(1)−Mo(2′)	152.2(5)
C(4)−C(3)−Mo(1)	168.9(7)	C(4)−C(3)−Mo(1′)	146.6(5)
C(6)−C(5)−Mo(2)	169.9(4)	C(6)−C(5)−Mo(1′)	146.9(4)
		C(6)A−C(5)A−Mo(2′)	153.7(4)
C(1)−C(2)−Si(1)	176.4(7)		
C(3)−C(4)−Si(2)	178.9(7)		
C(5)−C(6)−Si(3)	177.5(4)		

[a] Symmetry transformations used to generate equivalent atoms: (A) $x, -y + {}^1/_2, z$.

$(PMe_3)_4$ (2.268(1) Å)[3] is very nearly the average of those of $W_2(C{\equiv}CMe)_4(PMe_3)_4$ (2.276(1) Å, Table 3) and $W_2Cl_4(PMe_3)_4$ (2.262(1) Å),[17] suggesting, perhaps, that there is an additive relationship of the (subtle) effects of metal−alkynyl bonding on the metal−metal distance. The alkynyl ligands are nearly linear ($\angle$(C≡C−R) = 175[3]−177.9[4]°), but are bent back slightly from the M−C bond axis due to steric interactions with the PMe_3 ligands on the adjacent metal center ($\angle$(M−C≡C) = 165[2]−172.4[5]°).

We have previously proposed criteria for interpreting the M−C≡C−R bond distances of metal−alkynyl complexes in terms of the presence or absence of M−CCR π-interactions[1] and have noted that these distances typically are not known with sufficient precision from crystallographic data to allow unambiguous conclusions on this question to be drawn from them. The metrical data provided by the present structures are not exceptions in this latter regard, and we note only that the average C≡C bond distances (Table 6) are indistinguishable (at the 3σ confidence level) from each other and from the average for all metal−alkynyl complexes (1.201(16) Å),[1] and that, among the molybdenum complexes, the Mo−C bond distances (2.144[4]−2.16[2] Å) are slightly shorter than those for $Mo_2Me_4(PMe_3)_4$ (2.245[4] Å).[35] We have noted previously for $Mo_2(C{\equiv}CH)_4(PMe_3)_4$ (d(Mo−C) = 2.157[4] Å)[4] that the difference between the average Mo−CH_3 and Mo−CCH bond lengths (0.088 Å) is not statistically distinguishable from the 0.08 Å difference between the single-bond covalent radii of sp- and sp^3-hybridized carbon atoms and, therefore, that the π(CC)−δ(MM)−π(CC) conjugation that is evident from spectroscopic probes[2−4,6] cannot be detected at the resolution of the crystal structure; the present data do not alter this interpretation. It is regrettable that the metal−alkynyl bond distances for $W_2(C{\equiv}CMe)_4(PMe_3)_4$ are not of higher precision, because comparisons to the bond distances of $Mo_2(C{\equiv}CMe)_4(PMe_3)_4$ are potentially informative as to the nature of the M−CCR π-interactions due to the different d-orbital energies of molybdenum and tungsten. Crystal structures were determined for four different crystals of $W_2(C{\equiv}CMe)_4(PMe_3)_4$; the data reported herein are the highest quality among these and reflect the recurrent problem of decomposition of the crystals during the diffraction experiments.

The implication of the structural data for $Mo_2(C{\equiv}CR)_4(PMe_3)_4$ complexes regarding their vibrational spectra is that the close similarities among the core bond distances and bond angles of these complexes should be reflected in the frequencies of the corresponding stretching and bending modes, to the extent that those oscillators are uncoupled from each other. In particular, the narrow range spanned by the metal−metal bond lengths of these and related $Mo_2X_4(PMe_3)_4$ (X = Cl, Br, I) derivatives (Table 6) leads to the prediction that the zero-order metal−metal stretching frequencies of these compounds should exhibit a similarly narrow distribution.

(33) Chisholm, M. H.; Folting, K.; Huffman, J. C.; Putilina, E. F.; Streib, W. H.; Tatz, R. J. *Inorg. Chem.* **1993**, *32*, 3771−3780.
(34) Cotton, F. A.; Matusz, M. *Inorg. Chem.* **1988**, *27*, 2127−2131.
(35) Cotton, F. A.; Wiesinger, K. J. *Inorg. Chem.* **1990**, *29*, 2594−2599.

Table 5. Selected Bond Distances (Å) and Angles (deg) for $Mo_2(C{\equiv}CBu^t)_4(PMe_3)_4$

major-occupancy dimer		minor-occupancy dimer 1		minor-occupancy dimer 2	
		Distances (Å)			
Mo(1)−Mo(2)	2.132(3)	Mo(1′)−Mo(2′)	2.127(8)	Mo(1″)−Mo(2″)	2.061(12)
Mo(1)−C(1)	2.146(19)	Mo(1′)−C(1)	2.24(2)	Mo(2″)−C(1)	2.16(2)
Mo(1)−C(3)	2.20(2)	Mo(2′)−C(3)	2.21(2)	Mo(1″)−C(3)	2.21(2)
Mo(2)−C(5)	2.16(2)	Mo(1′)−C(5)	2.34(2)	Mo(1″)−C(5)	2.41(2)
Mo(2)−C(7)	2.12(2)	Mo(2′)−C(7)	2.28(2)	Mo(2″)−C(7)	2.30(3)
Mo(1)−P(1)	2.495(5)	Mo(2′)−P(1)	2.465(7)	Mo(2″)−P(1)	2.413(10)
Mo(1)−P(2)	2.490(5)	Mo(1′)−P(2)	2.388(8)	Mo(1″)−P(2)	2.394(10)
Mo(2)−P(3)	2.484(5)	Mo(1′)−P(3)	2.562(8)	Mo(2″)−P(3)	2.524(10)
Mo(2)−P(4)	2.505(5)	Mo(2′)−P(4)	2.473(7)	Mo(1″)−P(4)	2.588(10)
C(1)−C(2)	1.23(2)				
C(2)−C(9)	1.47(3)				
C(3)−C(4)	1.16(2)				
C(4)−C(13)	1.53(3)				
C(5)−C(6)	1.21(2)				
C(6)−C(17)	1.49(3)				
C(7)−C(8)	1.26(3)				
C(8)−C(21)	1.50(3)				
		Angles (deg)			
Mo(2)−Mo(1)−C(1)	108.4(6)	Mo(2′)−Mo(1′)−C(1)	100.6(6)	Mo(1″)−Mo(2″)−C(1)	100.4(6)
Mo(2)−Mo(1)−C(3)	108.8(5)	Mo(1′)−Mo(2′)−C(3)	99.3(6)	Mo(2″)−Mo(1″)−C(3)	102.8(7)
Mo(1)−Mo(2)−C(5)	105.7(6)	Mo(2′)−Mo(1′)−C(5)	100.1(6)	Mo(2″)−Mo(1″)−C(5)	100.3(6)
Mo(1)−Mo(2)−C(7)	104.1(7)	Mo(1′)−Mo(2′)−C(7)	99.7(6)	Mo(1″)−Mo(2″)−C(7)	100.5(7)
Mo(2)−Mo(1)−P(1)	105.90(17)	Mo(1′)−Mo(2′)−P(1)	103.2(3)	Mo(1″)−Mo(2″)−P(1)	104.0(4)
Mo(2)−Mo(1)−P(2)	105.34(19)	Mo(2′)−Mo(1′)−P(2)	107.0(3)	Mo(2″)−Mo(1″)−P(2)	108.0(4)
Mo(1)−Mo(2)−P(3)	101.70(17)	Mo(2′)−Mo(1′)−P(3)	105.0(3)	Mo(1″)−Mo(2″)−P(3)	106.1(4)
Mo(1)−Mo(2)−P(4)	102.16(16)	Mo(1′)−Mo(2′)−P(4)	105.5(3)	Mo(2″)−Mo(1″)−P(4)	105.8(4)
C(1)−Mo(1)−C(3)	142.7(8)	C(1)−Mo(1′)−C(5)	158.6(8)	C(1)−Mo(2″)−C(7)	159.1(9)
C(5)−Mo(2)−C(7)	150.2(10)	C(3)−Mo(2′)−C(7)	160.9(8)	C(3)−Mo(1″)−C(5)	156.4(8)
P(1)−Mo(1)−P(2)	148.7(3)	P(2)−Mo(1′)−P(3)	147.9(3)	P(2)−Mo(1″)−P(4)	145.8(4)
P(3)−Mo(2)−P(4)	156.1(2)	P(1)−Mo(2′)−P(4)	151.3(3)	P(1)−Mo(2″)−P(3)	149.9(4)
C(2)−C(1)−Mo(1)	164.2(17)	C(2)−C(1)−Mo(1′)	153(2)	C(2)−C(1)−Mo(2″)	155(2)
C(4)−C(3)−Mo(1)	163.8(17)	C(4)−C(3)−Mo(2′)	156(2)	C(4)−C(3)−Mo(1″)	153(2)
C(6)−C(5)−Mo(2)	169.3(18)	C(6)−C(5)−Mo(1′)	149(2)	C(6)−C(5)−Mo(1″)	148(2)
C(8)−C(7)−Mo(2)	163.8(17)	C(8)−C(7)−Mo(2′)	151.8(19)	C(8)−C(7)−Mo(2″)	152(2)
C(1)−C(2)−C(9)	174(2)				
C(3)−C(4)−C(13)	175(2)				
C(5)−C(6)−C(17)	175(2)				
C(7)−C(8)−C(21)	177(2)				

Table 6. Average $M_2X_4P_4$ Bond Distances (Å) and Bond Angles (deg) for $M_2X_4(PMe_3)_4$ Complexes[a]

	$Mo_2X_4(PMe_3)_4$						$W_2X_4(PMe_3)_4$		
nuclei	lit.[b]	$(C{\equiv}CH)_4$[c]	$(C{\equiv}CMe)_4$[d]	$(C{\equiv}CSiMe_3)_4$[d,e]	$(C{\equiv}CBu^t)_4$[d,e]	$(C{\equiv}CPr^i)_4$[e,f]	Cl_4[g]	$(C{\equiv}CMe)_4$[d]	$(C{\equiv}CMe)_2Cl_2$[h]
M−M	2.110(5)−2.218(2)	2.134(1)	2.1406[8]	2.135(1)	2.132(3)	2.10(1)	2.262(1)	2.2760[8]	2.268(1)
M−P	2.444[3]−2.565[2]	2.512[1]	2.508[1]	2.511[2]	2.494[5]	2.50[1]	2.508[2]	2.490[3]	2.484[3],[i] 2.503[3][j]
M−C		2.157[4]	2.144[4]	2.152[5]	2.16[2]	2.35[4]		2.124[9]	2.132[1]
C≡C		1.179[6]	1.197[5]	1.209[8]	1.22[2]	1.10[6]		1.19[1]	1.21[1]
C−R		0.93[4]	1.475[5]	1.811[6]	1.50[3]	1.50[8]		1.48[1]	1.45[2]
M−M−P	96.7[3]−104.6[1]	103.2[1]	102.45[4]	103.8[5]	103.8[2]	105.0[5]	101.14[2]	101.00[7]	101.6[1],[i] 101.5[1][j]
M−M−C		110.3[1]	110.9[1]	108.7[1]	106.8[6]	105[1]		110.7[3]	110.1[3]
M−C≡C		171.8[4]	172.4[3]	168.5[6]	165[2]	160[4]		172.4[5]	174[1]
C≡C−R		169[2]	177.9[4]	177.6[7]	175[3]	169[5]		177.3[6]	176[1]

[a] Esd's (standard deviations) are given in parentheses. Values in square brackets are arithmatic means of esd's. [b] X = F (ref 28), Cl (ref 17), Br (ref 10), I (ref 10), Me (ref 35), NCO (ref 34), NCS (ref 34), OCH_2Bu^t (ref 33). [c] Reference 4. [d] This work. [e] Values listed for major occupancy M_2 unit. [f] Reference 5. [g] Reference 17. [h] Reference 3. [i] $W(C{\equiv}CMe)_2(PMe_3)_2$ fragment. [j] $WCl_2(PMe_3)_2$ fragment.

Vibrational Modes of $M_2(C{\equiv}CR)_4(PMe_3)_4$ Complexes: Symmetry Considerations. Before presenting and discussing the vibrational spectra of $M_2(C{\equiv}CR)_4(PMe_3)_4$ complexes, we first briefly describe the types and symmetries of vibrational modes expected from group-theoretical considerations. The parent dimetallatetrayne, $Mo_2(C{\equiv}CH)_4(PMe_3)_4$, possesses 192 degrees of vibrational freedom, of which 48 are associated with the $Mo_2(CCH)_4P_4$ core. These 48 degrees of freedom can be described by 36 normal modes in D_{2d} symmetry, of which 18 ($5a_1 + a_2 + 2b_1 + 4b_2 + 6e$) are common with $M_2X_4(PMe_3)_4$ (X = halide) complexes. Valence-coordinate descriptions of these latter modes ($\nu_1-\nu_{18}$) have been set out in detail in a prior report,[20] and we retain the earlier descriptions and mode-numbering scheme in the present work. The other 18 normal modes of the $Mo_2(CCH)_4P_4$ core ($\nu_{19}-\nu_{36}$, $4a_1 + 2a_2 + 2b_1 + 4b_2 + 6e$) are associated with the stretching and bending motions of the ethynyl ligands; valence coordinates and selection rules for these modes are set out in Table 7. All but the two a_2-symmetry bending modes (λ_{op}(MCC), λ_{op}(CCH)) are expected to be Raman active and, thus, potentially observable by the resonance-Raman and FT-Raman measurements employed in this study. Replacing the terminal hydrogen atoms of the ethynyl ligands with methyl groups ($Mo_2(C{\equiv}CMe)_4(PMe_3)_4$, $W_2(C{\equiv}CMe)_4(PMe_3)_4$) or AMe_3 groups ($Mo_2(C{\equiv}CSiMe_3)_4(PMe_3)_4$, $Mo_2(C{\equiv}CBu^t)_4(PMe_3)_4$) does not change the number or valence-coordinate description of the core modes but increases the

Table 7. Symmetry Coordinates for the D_{2d}-Symmetry $M_2(C{\equiv}CH)_4P_4$ Skeleton[a]

description	no.	species	act.[b]
ν(C≡C)	ν_{19}	a_1	R
ν(≡CH)	ν_{20}	a_1	R
λ_{ip}(MCC)[c]	ν_{21}	a_1	R
λ_{ip}(CCH)[c]	ν_{22}	a_1	R
λ_{op}(MCC)[c]	ν_{23}	a_2	
λ_{op}(CCH)[c]	ν_{24}	a_2	
λ_{op}(MCC)[c]	ν_{25}	b_1	R
λ_{op}(CCH)[c]	ν_{26}	b_1	R
ν(C≡C)	ν_{27}	b_2	R, IR
ν(≡CH)	ν_{28}	b_2	R, IR
λ_{ip}(MCC)[c]	ν_{29}	b_2	R, IR
λ_{ip}(CCH)[c]	ν_{30}	b_2	R, IR
ν(C≡C)	ν_{31}	e	R, IR
ν(≡CH)	ν_{32}	e	R, IR
λ_{ip}(MCC)[c]	ν_{33}	e	R, IR
λ_{ip}(CCH)[c]	ν_{34}	e	R, IR
λ_{op}(MCC)[c]	ν_{35}	e	R, IR
λ_{op}(CCH)[c]	ν_{36}	e	R, IR

[a] Descriptions of modes $\nu_1-\nu_{18}$ are provided in Table 2 and Figure 1 of ref 20. [b] R = Raman, IR = infrared. [c] The subscripts ip and op denote in-plane and out-of-plane motion relative to the CMC plane.

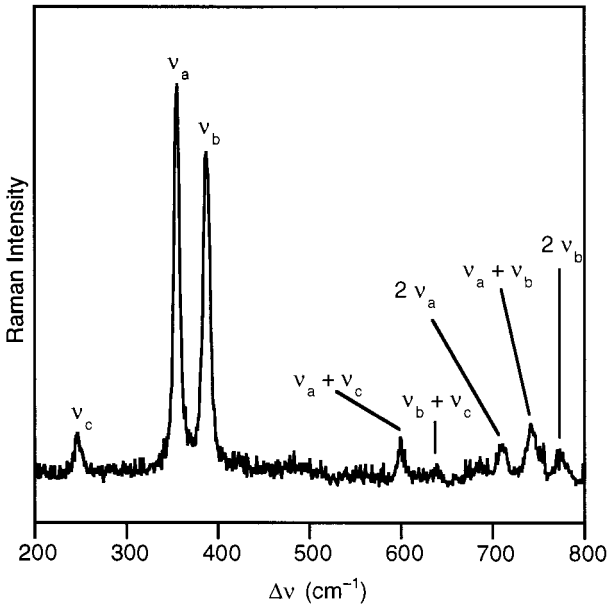

Figure 5. Resonance-Raman spectrum of $Mo_2(^{13}C{\equiv}^{13}CSiMe_3)_4(PMe_3)_4$ in THF solution at 293 K (λ_{max} $^1(\delta\rightarrow\delta^*)$ = 692 nm, λ_{ex} = 632.8 nm).

number of vibrational degrees of freedom to 228 and 336, respectively, leading to the expectation (borne out experimentally, vide infra) that the vibrational spectra of these species will increase correspondingly in complexity.

Resonance-Raman Spectra of $Mo_2(C{\equiv}CSiMe_3)_4(PMe_3)_4$ and Isotopomers. The resonance-Raman spectrum of $Mo_2(^{13}C{\equiv}^{13}CSiMe_3)_4(PMe_3)_4$ obtained upon excitation into the $^1(\delta\rightarrow\delta^*)$ absorption band is shown in Figure 5, and band wavenumbers and intensity and depolarization ratios for this compound, the natural-abundance compound, and the isotopomers $Mo_2(C{\equiv}CSiMe_3\text{-}d_9)_4(PMe_3)_4$ and $Mo_2(C{\equiv}CSiMe_3)_4(PMe_3\text{-}d_9)_4$ are set out in Table 8. Attempts to acquire resonance-Raman spectra for other $Mo_2(C{\equiv}CR)_4(PMe_3)_4$ complexes were unsuccessful because they are photochemically unstable in solution under the excitation conditions.

The resonance-Raman spectra of $Mo_2(C{\equiv}CSiMe_3)_4(PMe_3)_4$ and its isotopomers exhibit three resonance-enhanced bands, denoted ν_a, ν_b, and ν_c (Figure 5 and Table 8), that are attributable

Table 8. Resonance-Raman Data for $Mo_2(C{\equiv}CSiMe_3)_4(PMe_3)_4$ and Isotopomers in THF Solution at Room Temperature

band	NA[a]	$PMe_3\text{-}d_9$[c]	$^{13}C{\equiv}^{13}C$[c]	$C{\equiv}CSiMe_3\text{-}d_9$[c,d]
		Wavenumber (cm^{-1})		
ν_c	254[b]	252	247	
ν_a	362[b,e]	359 (ρ = 0.30)[f]	355 (ρ = 0.34)[f]	351
ν_b	397[b,e]	395 (ρ = 0.31)[f]	387 (ρ = 0.33)[f]	390
$\nu_a+\nu_c$	619[b]	604	599	
$\nu_b+\nu_c$			639	
$2\nu_a$	722[b]	720	710	
$\nu_a+\nu_b$	758[b]	755	741	
$2\nu_b$	795[b]		774	
		Intensity Ratio[f]		
ν_b/ν_a	0.45[b,g]	0.45	0.95	0.94
ν_c/ν_b	0.18[b]	0.15	0.11	
ν_c/ν_a	0.08[b]	0.07	0.11	

[a] NA = natural abundance. [b] λ_{ex} = 648.7 nm. [c] λ_{ex} = 632.8 nm. [d] Low-quality spectrum because of sample photodecomposition; only the two most intense features were well resolved. [e] For λ_{ex} = 632.8 nm, bands ν_a and ν_b are observed at 362 and 396 cm^{-1}, respectively; band ν_c is not observed. [f] Intensity and depolarization ratios are based upon integrated peak areas. [g] The ν_b/ν_a intensity ratio for λ_{ex} = 632.8 nm is 0.42.

to fundamental vibrations, together with a number of bands arising from overtones and combinations of them. These bands lie in the region 200−800 cm^{-1}; above this range a strong, rising background signal, attributed to fluorescence of the compound, obscures other Raman bands, including in the important C≡C stretching region.

Polarization data for $Mo_2(^{13}C{\equiv}^{13}CSiMe_3)_4(PMe_3)_4$ and $Mo_2(C{\equiv}CSiMe_3)_4(PMe_3\text{-}d_9)_4$ (Table 8) indicate that ν_a and ν_b arise from totally symmetric modes. Specifically, the depolarization ratios of ν_a and ν_b (ρ = 0.30−0.34; Table 8) are consistent with expectation (ρ = 1/3) for resonance with a dipole-allowed single-axis-polarized transition (e.g., $^1(\delta\rightarrow\delta^*)$), which should result in resonance enhancement of totally symmetric vibrations having normal coordinates associated with the excited-state distortion.[36] Band ν_c was too weak under our experimental conditions to allow determination of ρ, but both theoretical considerations and previous experimental results[10,37] suggest that it is also very likely to arise from a totally symmetric mode; the observation of combinations of ν_c with ν_a and ν_b (Figure 5), in particular, strongly supports this conclusion.[36,37]

The frequencies and intensities of bands ν_a, ν_b, and ν_c of $Mo_2(C{\equiv}CSiMe_3)_4(PMe_3)_4$ are highly sensitive to the isotopic composition of the alkynyl ligands. Relative to their frequencies for the natural-abundance compound (Table 8), all three bands are shifted strongly to lower frequency for $Mo_2(^{13}C{\equiv}^{13}CSiMe_3)_4(PMe_3)_4$ ($\Delta\nu_a$ = −7 cm^{-1}; $\Delta\nu_b$ = −10 cm^{-1}; $\Delta\nu_c$ = −7 cm^{-1}), while for $Mo_2(C{\equiv}CSiMe_3\text{-}d_9)_4(PMe_3)_4$ ν_a ($\Delta\nu_a$ = −11 cm^{-1}) and ν_b ($\Delta\nu_b$ = −7 cm^{-1}) also shift significantly to lower frequency; unfortunately, the quality of the spectrum of the latter compound was insufficient to allow observation of ν_c. The relative intensities of ν_a and ν_b are also strongly sensitive to labeling of the alkynyl ligands, differing by a factor of 2 between the natural-abundance compound ($I(\nu_b)/I(\nu_a)$ = 0.45) and the labeled compounds ($I(\nu_b)/I(\nu_a)$ = 0.95 (^{13}C), 0.94 ($SiMe_3\text{-}d_9$)). (The intensity ratios $I(\nu_a)/I(\nu_c)$ and $I(\nu_c)/I(\nu_b)$ may also be sensitive to isotopic labeling, but because ν_c is weak, these differences are near the limits of uncertainty set by the experimental error.) In contrast to these alkynyl-ligand isotope

(36) Myers, A. B.; Mathies, R. A. In *Biological Applications of Raman Spectroscopy, Vol. 2, Resonance Raman Spectra of Polyenes and Aromatics*; Spiro, T. G., Ed.; Wiley: New York, 1987; pp 1−58.
(37) Clark, R. J. H.; Stead, M. J. *Inorg. Chem.* **1983**, *22*, 1214−1220.

effects, the frequencies of bands ν_a, ν_b, and ν_c are largely insensitive to deuteration of the trimethylphosphine ligands, shifting by an amount (2−3 cm^{-1}) that approaches the uncertainty of the peak positions, and the intensity ratios of the bands are constant.

In our initial report on $Mo_2(C{\equiv}CSiMe_3)_4(PMe_3)_4$,[2] band ν_a was assigned to the ν_1 [a_1, $\nu(Mo_2)$] mode on the basis of the fact that it is the most strongly resonantly enhanced band, as is typically observed for $\nu(M_2)$ bands of quadruply bonded complexes,[37,38] and because of the close similarity of its frequency (362 cm^{-1}) to the $\nu(Mo_2)$ frequencies of $Mo_2X_4(PMe_3)_4$ (X = Cl, Br, I) complexes (342−355 cm^{-1}).[10] The metal−metal distance reported here for $Mo_2(C{\equiv}CSiMe_3)_4(PMe_3)_4$ (2.135(1) Å) is very similar to those of the $Mo_2X_4(PMe_3)_4$ complexes (2.125(1)−2.130(0) Å, Table 6), consistent with this assignment. Bands ν_b and ν_c were assigned to the ν_2 [a_1, ν(MoC)] and ν_3 [a_1, ν(MoP)] modes, respectively. In the case of ν_2 [a_1, ν(MoC)] there were no precedents involving dinuclear compounds on which to base this assignment, but the frequency is consistent with M−CCR stretching frequencies for other metal−alkynyl complexes.[1,39−43] The frequency of ν_3 [a_1, ν(MoP)] is similar to M−P stretching frequencies for benchmark complexes established by isotopic labeling.[44]

The resonance-Raman data reported here for isotopically labeled $Mo_2(C{\equiv}CSiMe_3)_4(PMe_3)_4$ point to two problems with our earlier assignments. First, the lack of a significant frequency shift of ν_c upon deuteration of the trimethylphosphine ligands, and the large shifts of ν_c upon ^{13}C and deuterium labeling of the alkynyl ligands, exclude the previous assignment of this band to ν(MoP), as well as to any phosphine-localized mode. Second, the observation that the resonance-Raman intensity ratio $I(\nu_b)/I(\nu_a)$ varies by a factor of 2 upon isotopic labeling of the alkynyl ligands strongly implicates vibrational mixing between the zero-order $\nu(Mo_2)$ and ν(MoC) modes to which ν_a and ν_b, respectively, had been assigned.[2]

This second point deserves elaboration. The resonance-Raman intensities yield information about the $^1(\delta{\rightarrow}\delta^*)$ excited-state distortions along the vibrational coordinates of the resonance-enhanced modes.[18,37,45] If the molecule distorts along several noncoupled vibrational modes in the excited state, then isotopic effects upon the frequencies of each of these modes should be distinct according to their particular nuclear motions, while effects upon relative intensities of their bands should be small: of the order of the percentage change in frequency.[36] If, on the other hand, the distortion is along a single internal coordinate (such as the metal−metal bond) that is distributed among a number of vibrational modes, then the bands for each of these modes will be proportionately resonance enhanced. In this case, the relative intensities of the bands may be very isotope sensitive because the potential-energy distributions (PEDs) of the modes

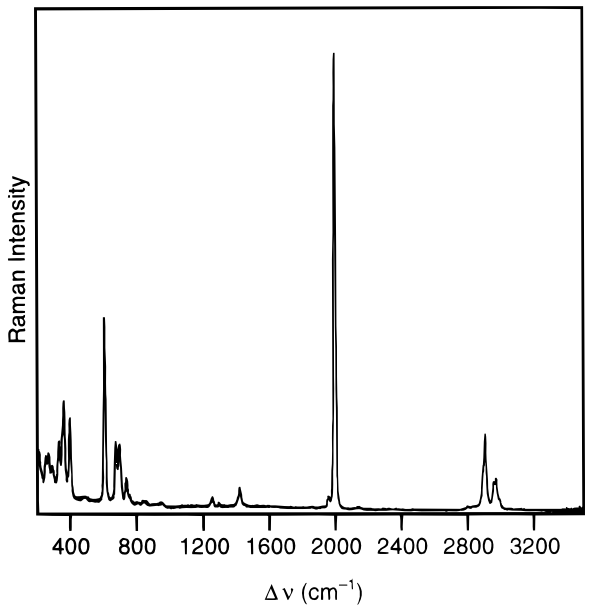

Figure 6. FT-Raman spectrum of polycrystalline $Mo_2(C{\equiv}CSiMe_3)_4(PMe_3)_4$ at 293 K.

can be very sensitive to frequency matches among the zero-order vibrations.[36,46] We conclude, therefore, that the modes assigned to ν_a and ν_b, while probably best described as $\nu(Mo_2)$ and ν(MoC), are strongly coupled, accounting for the isotopic sensitivity of both their frequencies and resonance-Raman intensities. The mode that gives rise to band ν_c is evidently also coupled with these modes, given that ν_c shifts similarly in frequency upon isotopic labeling; an assignment of ν_c that is consistent with these results is to the alkynyl bending mode ν_{21} [a_1, λ_{ip}(MCC)].

Normal-coordinate calculations (vide infra) were performed to determine the magnitude of the couplings among $\nu(Mo_2)$, ν(MoC), and ν_c. To provide the extensive set of vibrational frequencies required for these calculations, FT-Raman spectra were acquired of the $M_2(C{\equiv}CR)_4(PMe_3)_4$ complexes.

FT-Raman Spectra of $Mo_2(C{\equiv}CR)_4(PMe_3)_4$ and $Mo_2X_4(PMe_3)_4$ (X = Halide) Complexes. The FT-Raman spectrum (λ_{ex} = 1064 nm) of crystalline $Mo_2(C{\equiv}CSiMe_3)_4(PMe_3)_4$ is shown in Figure 6; band wavenumbers, intensities, and assignments for this compound and its isotopomers ($^{13}C{\equiv}^{13}CSiMe_3$, $C{\equiv}CSiMe_3$-d_9, PMe_3-d_9), for $Mo_2(C{\equiv}CH)_4(PMe_3)_4$ and isotopomers ($C{\equiv}CD$, PMe_3-d_9), and for $Mo_2(C{\equiv}CR)_4(PMe_3)_4$ (R = Me, Bu^t) and $W_2(C{\equiv}CMe)_4(PMe_3)_4$ are set out in Table 9. The FT-Raman spectrum of $Mo_2(C{\equiv}CSiMe_3)_4(PMe_3)_4$ exhibits more than 30 bands arising from fundamental vibrations, as compared to the three fundamental bands observed in the resonance-Raman spectrum. The region below 500 cm^{-1}, in which ν_a, ν_b, and ν_c lie and bands from $Mo_2C_4P_4$ core modes are expected, is particularly congested because bands from alkynyl- and phosphine-localized modes also lie in this region (vide infra).

The FT-Raman bands of $M_2(C{\equiv}CR)_4(PMe_3)_4$ complexes arising from alkynyl- and phosphine-localized modes have been identified and assigned on the basis of isotope-substitution data and through comparisons to reference compounds. For the alkynyl modes, there are extensive literature assignments of the vibrational spectra of terminal acetylenes and iodoacetylenes ($HC{\equiv}CH/D$,[47] $HC{\equiv}CI$,[48] $H/DC{\equiv}CCH_3/D_3$,[49] $IC{\equiv}CCH_3$,[25] $HC{\equiv}$

(38) Cotton, F. A.; Walton, R. A. *Multiple Bonds between Metal Atoms*; Clarendon: Oxford, 1993; pp 732−738.
(39) Ballester, L.; Cano, M.; Santos, A. *J. Organomet. Chem.* **1982**, *229*, 101−107.
(40) Masai, H.; Sonogashira, K.; Hagihara, N. *J. Organomet. Chem.* **1971**, *26*, 271−276.
(41) Sonogashira, K.; Fujikura, Y.; Yatake, T.; Toyoshima, N.; Takahashi, S.; Hagihara, N. *J. Organomet. Chem.* **1978**, *145*, 101−108.
(42) Klein, H.-F.; Beck-Hemetsberger, H.; Reitzel, L.; Rodenhäuser, B.; Cordiear, G. *Chem. Ber.* **1989**, *122*, 43−51.
(43) Barral, M. C.; Jimenez, R.; Royer, E.; Moreno, V.; Santos, A. *Inorg. Chim. Acta* **1978**, *31*, 165−169.
(44) Nakamoto, K. *Infrared and Raman Spectra of Inorganic and Coordination Compounds*, 5th ed.; Wiley-Interscience: New York, 1997; Part B, pp 195−199.
(45) Ceylan, V. K.; Sourisseau, C.; Brencic, J. V. *J. Raman Spectrosc.* **1985**, *16*, 128−136.
(46) Wilson, E. B., Jr.; Decius, J. C.; Cross, P. C. *Molecular Vibrations*; McGraw-Hill: New York, 1955.

Table 9. FT-Raman Wavenumbers (cm^{-1}) of Vibrational Modes for $Mo_2(C{\equiv}CR)_4(PMe_3)_4$ Complexes[a]

	$Mo_2(C{\equiv}CH)_4(PMe_3)_4$			$Mo_2(C{\equiv}CSiMe_3)_4(PMe_3)_4$				$M_2(C{\equiv}CR)_4(PMe_3)_4$		
mode	NA[b]	C≡CD	PMe_3-d_9	NA[b]	$^{13}C{\equiv}^{13}C$	PMe_3-d_9	$SiMe_3$-d_9	Mo, C≡CMe	W, C≡CMe	Mo, C≡CBu^t
$\tau(CH_3)$[c]				160(m),[e] 200(m)	170(m),[e] 208(m)	172(w), 195(m)	155(w),[e] 180(w)[e]	168(w)	168(m)	160(vw,sh),[e] 185(vw,sh)
$\tau(CH_3)$[d]	180(w,br)[e]	165(w), 190(w)	175(w)	140(w,sh), 160(m)[e]	140(w), 170(m)[e]	142(m)[e]	155(w),[e] 180(w)[e]	200(w, sh)	200(vw)	160(vw,sh),[e] 170(w)
ν(MP)	230(vw)	225(m)	233(w)	225(w,sh)	225(w,sh)	231(m)[e]	220(w)	*f*	*f*	227(m)
$\lambda(MCC)_{asym}$			268(w)[h]							
ν_c	299(w)	285(w,sh)	303(w)	253(m)	248(m)	253(m)	234(w)[e]	*f*	*f*	280(m)
$\delta(CPC)_{asym}$	270(m)	271(m)	259(m)[h]	269(m)	270(m)	231(m)[e]	264(w)[e]	274(w)[g]	273(w)[g]	268(m), 280(m)[h]
$\delta(CAC)_{sym}$[c,i]				292(w)	291(m)	291(w)	264(w)[e]			445(m,sh), 452(s)
λ(CCR)	540(w), 599(w)	476(m), 494(m)	538(w), 597(w)	331(m)	331(m)	338(s)[e]	314(m)	326(m)	314(s)	330(vvw), 303(w)
$\delta(CPC)_{sym}$	357(w)	357(m)	344(m)	352(m,sh)	351(m,sh)	338(s)[e]	352(m)[e]	363(m)[e]	342(w)	359(m)[e]
ν_a	387(m)	386(s)	389(s)	361(s)	358(s)	362(s)	352(m)[e]	363(m)[e]	*f*	359(m)[e]
$\nu(MC)_{asym}$	*f*	*f*	*f*	385(vw,sh)	*f*	385(vw,sh)	373(vw,sh)	405(m,sh)[h]	*f*	*f*
ν_b	421(m)	414(s)	422(s)	398(s)	391(s)	397(s)	392(m)	386(s)	388(m)	380(s)
$\delta(CAC)_{asym}$[i]										537(m)
$\nu(AMe_3)_{asym}$[i]				606(vs)	601(vs)	606(vs)	546(s)			1201(m)
$\nu(AMe_3)_{sym}$[i]							641(m)			920(w)
$\nu(PC)_{sym}$	678(m)	679(s)	613(s)	673(m)	675(s)		673(m)	674(m)	675(m)	671(s)
$\nu(PC)_{asym}$	739(m)	739(w)	680(w)	738(w)	738(w)	679(vw,sh), 635(w)	737(w)	737(m)	737(w)	727(vs)
δ(ACH)[i]				695(m), 757(vw), 805(vvw)	675(m),[e] 691(m,sh), 757(vvw,sh)	694(m)	641(m)			
$\rho(CH_3)$[d]	952(vw)		770(w)	849(vw,br), 953(vw,br)	1086(w)	770(vw)[e]		943(vvw), 964(m), 973(s)		902(vw)
$\delta(HCH)_{sym}$[c]				1246(vvw,sh), 1257(vw)	1245(vvw,sh), 1255(w)	1247(vvw,sh), 1257(vw)		1371(m)	1374(m)	1241(w), 1384(w)
$\delta(CH)_{sym}$[d]		1303(vvw)		1297(vw)	1295(vvw)		1295(vvw)			1291(vw)
$\delta(HCH)_{asym}$[c]				1411(vw,sh)	1410(vw,sh)	1411(vw)	990(w)			1450(m)
$\delta(CH)_{asym}$[d]	1421(m)	1422(m), 1449(vw)	1008(vw), 1022(w), 1039(w)	1422(w)	1422(w)	1016(vw), 1037(vw)	1420(w)	1419(m)	1423(m)	1418(m)
$\nu_{19}(^{13}C{\equiv}^{13}C)$[j]					1918(vs,sh), 1922(vs)					
$\nu^{19}(^{13}C{\equiv}^{12}C)$[j]	1874(w)		1872(w), 1883(w)	1961(w)	1960(w)	1960(w)	1960(w)			2016(w,sh), 2027(w)
$\nu_{19}(^{12}C{\equiv}^{12}C)$[j]	1909(vvs)	1800(vvs,sh), 1804(vvs)	1909(vs,sh), 1910(vvs)	1995(vvs,sh), 1999(vvs)		1994(vvs,sh), 2000(vvs)	1994(vvs,sh), 1998(vvs)	2070(vvs)	2064(vvs)	2060(vvs)[l]
2*$\delta(CH)_{asym}$[d]				2801(vw), 2842(vw,br)	2800(vvw)		2789(vvw)		2845(w)	2697(w), 2760(w), 2797(w), 2822(w)
$\nu(CH)_{sym}$[c]				2896(m,sh)	2897(m,sh)	2897(m)	2112(s)	2849(w)	2845(w)	2860(m)
$\nu(CH)_{sym}$[d]	2908(s)	2900(m,sh), 2907(s)	2126(s)	2907(s)	2907(s)	2122(s)	2905(s)	2901(s)	2902(s)	2903(vs)
$\nu(CH)_{asym}$[c]				2958(m)	2958(m)	2960(m)	2212(m)	*k*	*k*	2943(m)
$\nu(CH)_{asym}$[d]	2973(s)	2964(w), 2978(m), 3005(w)	2225(m,sh), 2230(m), 2246(w)	2972(m), 2991(w,sh)	2972(m)	2227(m), 2245(w)	2971(m), 2991(vw,sh)	2970(m)	2970(m)	2967(vs), 2988(m,sh)
ν(≡CH)	*m*	2510(vw), 2530(vw)	3242(vw), 3269(vw)							

[a] Relative intensities are normalized to the strongest ν(C≡C) band (vvs). [b] NA = natural abundance. [c] CCR mode. [d] PMe_3 mode. [e] Probable overlap with other bands. [f] Not resolved. [g] The feature assigned to $\delta(CPC)_{asym}$ appears to be composite, and ν_c may lie in this region. [h] Assignment uncertain. [i] A = Si (for $SiMe_3$) or C (for Bu^t). [j] Weak bands in the ν(C≡C) region are probably Fermi resonances or hot bands. The pronounced shoulder of the $SiMe_3$ compounds may result from a site splitting. [k] Obscured by PMe_3 bands. [l] Additional weak features at 2144 and 1965 cm^{-1} are presumably combinations. [m] Not observed. Bands at 3270 and 3245 cm^{-1} are observed in the infrared spectrum of a THF solution.

Table 10. Assigments of Selected FT-Raman Bands (cm^{-1}) for $Mo_2X_4(EMe_3)_4$ Complexes

				$Mo_2Cl_4(EMe_3)_4$			$Mo_2Br_4(EMe_3)_4$		$Mo_2I_4(EMe_3)_4$	
mode	PMe_3[a]	PMe_3-d_9[a]	$AsMe_3$[a]	PMe_3	PMe_3-d_9	$AsMe_3$	PMe_3	PMe_3-d_9	PMe_3	PMe_3-d_9
ν_1 [a_1, ν(MM)]				353(w)[b]	354(vw)	351(vw)	351(w)[b]	352(w)	343(w)[b]	343(w)
ν_{10} [e, ν(MX)]				332(vvw)[b]	342(w)	337(vw)	279(w)[b]	270(w)	177(m)	177(w)
ν_6 [b_2, ν(MX)]				277(m)[c]	275(m)[c]	279(w)[c]	188(w)	184(m)	125(w)[d]	125(w)[d]
ν_2 [a_1, ν(MX)]				277(m)[c]	275(m)[c]	279(w)[c]	158(w,sh)	160(w)	105(w)[d]	102(w)[d]
$\delta(CEC)_{sym}$	315(w)	269(w)	265(vw)	353(w)[b]	308(vw)	279(m)[b]	351(w)[b]	315(w)	343(w)[b]	313(vw)
$\delta(CEC)_{asym}$	288(w), 269(w)	242(w), 224(w)	249(w), 222(vw)	277(m)[b]	231(m)[b]	228(m)[b]	279(w)[b]	234(w)[b]	285(w)	238(w,sh)
ν_3 [a_1, ν(ME)]				237(vw)	231(m)	228(m)[b]	228(vw)	234(w)[b] 212(vw)	250(w)	250(w) 214(vw)
$\tau(CH_3)$[g]	224(vw), 210(vw,sh)	164(vw), 152(vw,sh)	196(w), 174(w)	190(w),[f] 155(w)	179(w),[f] 153(vw)	*e*	188(w)[f]	146(vw)	200(w,sh)	160(w,sh)

[a] References 55 and 56. [b] Observed features are composites of bands due to ligand modes and core mode(s). [c] The a_1 and b_2 components of ν(MoCl) are not individually resolved. [d] Possibly composite of bands due to ν(MoI) and Mo−P bending modes. [e] Probably included in the broad 228 cm^{-1} feature. [f] Frequency derived from PMe_3/PMe_3-d_9 difference spectrum. [g] Assignments for metal complexes are based on low-temperature data for EMe_3 (refs 55 and 56); the higher and lower frequencies of the two bands that are observed in some cases correlate to the e- and a_2-symmetry torsion modes of EMe_3. See also ref 57.

CBu^t,[50] IC≡CBu^t,[50] H/DC≡$CSiMe_3$,[51−53] IC≡$CSiMe_3$[54]) on which to base assignments. The most prominent band arising from an alkynyl mode is due to the a_1-symmetry C≡C stretch (ν_{19}), which is the most intense band in the spectra of these complexes (Figure 6). Assignments for other alkynyl modes are discussed later in the paper in the context of specific compounds.

For the phosphine-localized modes, benchmarks for the frequencies and relative intensities (under nonresonance conditions) of bands are provided by FT-Raman spectra of compounds of the type $Mo_2X_4(PMe_3)_4$ (X = Cl, Br, I), which have been the prior subjects of comprehensive resonance-Raman[10] and far-infrared[19,20] spectroscopic studies, and of their deuterated isotopomers. Frequencies for the phosphine-localized modes and selected $Mo_2X_4E_4$ core modes (assignments for which are based on prior work)[10,20] are set out in Table 10; the latter are numbered according to the scheme used in prior work.[20] These compounds exhibit bands attributable to three low-frequency (ν < 500 cm^{-1}) phosphine-localized modes: the symmetric (∼350 cm^{-1}) and asymmetric (∼275 cm^{-1}) δ(CPC) deformations, and methyl torsion (∼200 cm^{-1}),[55−57] as established by comparisons among spectra of natural-abundance and deuterated (PMe_3-d_9) derivatives and of the spectra of $Mo_2Cl_4(PMe_3)_4$ and $Mo_2Cl_4(AsMe_3)_4$ (Table 10). For example, deuteration of $Mo_2Br_4(PMe_3)_4$ shifts $\delta(CPC)_{sym}$ from 351 to 315 cm^{-1}, revealing ν_1 [a_1, $\nu(Mo_2)$] as an underlying feature at 351 cm^{-1},[58] while $\delta(CPC)_{asym}$ shifts from 279 to 234 cm^{-1} and $\tau(CH_3)$ shifts from 188 to 146 cm^{-1} (Figure 7). Bands attributable to ν_2 [a_1, ν(MoX)] and a M−P stretching mode are also observed, although neither is prominent.[59] For $Mo_2Cl_4(PMe_3)_4$, the situation is particularly complicated because both δ(CPC) bands are nearly superimposed upon ν(MoCl) bands. The phosphine bands exhibit considerably higher intensities relative to the $Mo_2X_4P_4$ core modes in FT-Raman spectra than they exhibit in resonance-Raman spectra, in which the intensity for bands arising from PMe_3 modes is negligible.

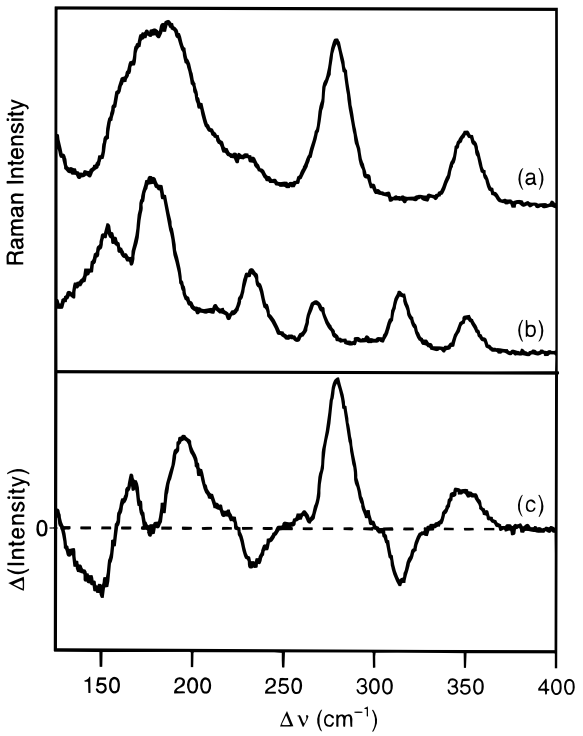

Figure 7. FT-Raman spectra of polycrystalline $Mo_2Br_4(PMe_3)_4$ and d_{36}-isotopomer at 293 K: (a) $Mo_2Br_4(PMe_3)_4$; (b) $Mo_2Br_4(PMe_3$-$d_9)_4$; (c) difference spectrum (a − b). The intensities are normalized so that the ν(CH)/ν(CD) bands (not shown) are of equal intensity.

(47) Herzberg, G. *Molecular Spectra and Molecular Structure II. Infra-Red and Raman Spectra of Polyatomic Molecules*; Van Nostrand: New York, 1945; pp 180−181.
(48) Rogstad, A.; Cyvin, S. J. *J. Mol. Struct.* **1974**, *20*, 373−379.
(49) Christensen, M. T.; Thompson, H. W. *Trans. Faraday Soc.* **1956**, *52*, 1439−1450.
(50) Hüttner, W.; Zeil, W. *Z. Naturforsch.* **1970**, *25a*, 1281−1291.
(51) The assignments for HC≡$CSiMe_3$ in the ν < 1000 cm^{-1} region are less secure than those of the other alkynes; two different, detailed sets of assignments have been reported in the literature (refs 52 and 53).
(52) Buchert, H.; Zeil, W. *Z. Phys. Chem. Neue Folge* **1961**, *29*, 317−328.
(53) Nikitin, V. S.; Polyakova, M. V.; Baburina, I. I.; Belyakov, A. V.; Bogoradovskii, E. T.; Zovgorodnii, V. S. *Spectrochim. Acta* **1990**, *46a*, 1669−1667.
(54) Buchert, H.; Zeil, W. *Spectrochim. Acta* **1962**, *18*, 1043−1053.
(55) Rojhantalab, H.; Nibler, J. W.; Wilkins, C. J. *Spectrochim. Acta* **1976**, *32a*, 519−533.
(56) Rojhantalab, H.; Nibler, J. W. *Spectrochim. Acta* **1976**, *32a*, 947−956.
(57) Schneider, W.; Thiel, W.; Komornicki, A. *J. Phys. Chem.* **1988**, *92*, 5611−5619.
(58) That the ν_1 [a_1, $\nu(Mo_2)$] band is relatively weak for 1064 nm (nonresonance) excitation is general for compounds of this type; we have also found a similar relative intensity of $\nu(M_2)$ for $K_4[Mo_2Cl_8]$.
(59) Only one broad line attributable to ν(Mo−P) is observed near 225−240 cm^{-1}; normal-coordinate calculations (vide infra) suggest that splittings among the a_1-, b_2-, and e-symmetry components of ν(MoP) are much smaller than are those among the ν(MoX) modes. The apparent lack of a frequency shift of this band upon deuteration arises because the band is too weak for the maximum to be reliably identified.

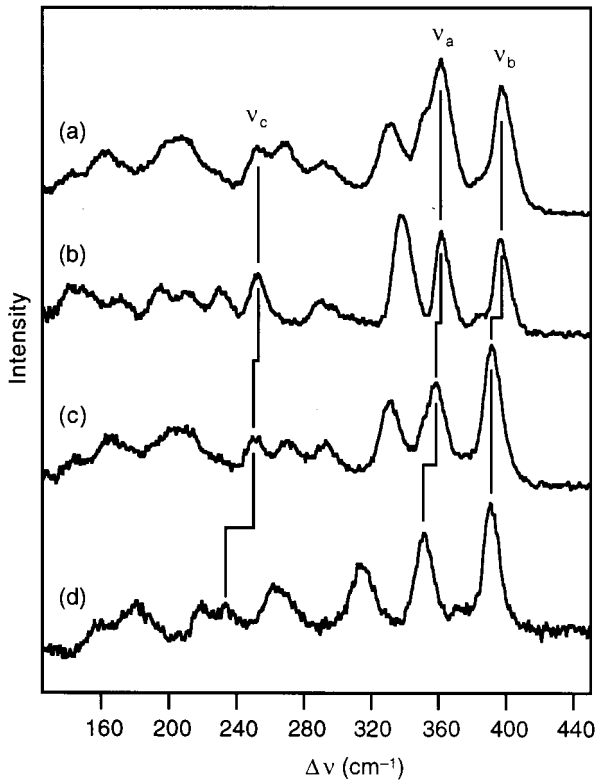

Figure 8. FT-Raman spectra of polycrystalline $Mo_2(C{\equiv}CSiMe_3)_4(PMe_3)_4$ and isotopomers at 293 K: (a) $Mo_2(C{\equiv}CSiMe_3)_4(PMe_3)_4$; (b) $Mo_2(C{\equiv}CSiMe_3)_4(PMe_3\text{-}d_9)_4$; (c) $Mo_2(^{13}C{\equiv}^{13}CSiMe_3)_4(PMe_3)_4$; (d) $Mo_2(C{\equiv}CSiMe_3\text{-}d_9)_4(PMe_3)_4$.

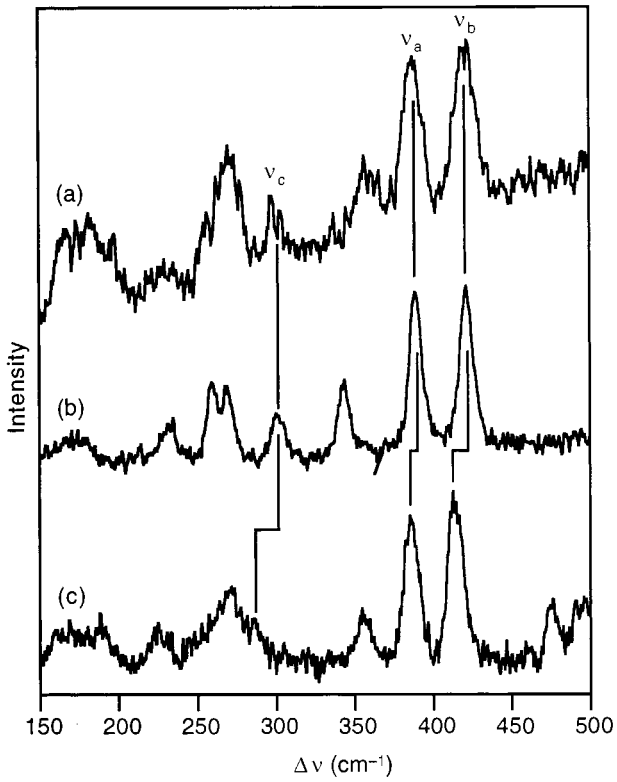

Figure 9. FT-Raman spectra of polycrystalline $Mo_2(C{\equiv}CH)_4(PMe_3)_4$ and isotopomers at 293 K: (a) $Mo_2(C{\equiv}CH)_4(PMe_3)_4$; (b) $Mo_2(C{\equiv}CH)_4(PMe_3\text{-}d_9)_4$; (c) $Mo_2(C{\equiv}CD)_4(PMe_3)_4$.

Band assignments for the phosphine-localized modes of $M_2(C{\equiv}CR)_4(PMe_3)_4$ compounds follow straightforwardly, for the most part, from comparisons to the halide analogues (Table 10) and to the PMe_3-d_9 labeled derivatives (Table 9). The $Mo_2(C{\equiv}CSiMe_3)_4(PMe_3)_4$ isotopomers afforded the highest-quality FT-Raman spectra because of their relatively high thermal stability (allowing for higher laser powers and longer data-acquisition times); these spectra form the basis for assigning the core vibrational modes of the other $M_2(C{\equiv}CR)_4(PMe_3)_4$ complexes. As shown in Figure 8, the spectra exhibit features corresponding well in frequency to bands ν_a, ν_b, and ν_c of the resonance-Raman spectra (Figure 5). The ν_a band is superimposed with the $\delta(CPC)_{sym}$ band in the natural-abundance compound but is clearly observed in the PMe_3-d_9 derivative, for which the phosphine-localized band is shifted to lower frequency. The feature attributed to ν_b may be a composite consisting of more than one ν(MoC)-derived vibrational transition. The only other feature attributable to a ν(MoC) mode is very weak and is assigned to a nontotally symmetric stretch (b_2 symmetry, ν_6, or e symmetry, ν_{10}), denoted $\nu(MC)_{asym}$ (Table 9).

It must be admitted that the FT-Raman spectra are sufficiently complex that assignments of ν_a, ν_b, and ν_c (particularly the latter) would be difficult without the comparisons to the resonance-Raman data. There are several additional low-frequency features in the FT-Raman spectra that, like ν_a, ν_b, and ν_c, are sensitive to isotopomeric substitution on the $C{\equiv}CSiMe_3$ ligands, but none of these is observed in the resonance-Raman spectra. For example, the 150−200 cm^{-1} region changes drastically upon deuteration of the $SiMe_3$ group (Figure 8), which is the result of the shifts of $\tau(CH_3)$ modes to lower frequency.[55,56] There are two torsion modes (symmetric and asymmetric) each for the $SiMe_3$ and PMe_3 groups that are split by as much as 20−30 cm^{-1},[55,57] and our assignments assume overlapping bands. A more distinct isotope-sensitive band is located at 331 cm^{-1} (natural abundance), which shifts to 314 cm^{-1} for the $SiMe_3$-d_9 derivative (Figure 8). This is reasonably assigned to a λ(CCSi) mode by comparison to the frequency of 350 cm^{-1} for the analogous mode of $HC{\equiv}CSiMe_3$.[53]

The FT-Raman spectra of $Mo_2(C{\equiv}CMe)_4(PMe_3)_4$, $Mo_2(C{\equiv}CBu^t)_4(PMe_3)_4$, and $W_2(C{\equiv}CMe)_4(PMe_3)_4$ are assigned by analogy to those of $Mo_2(C{\equiv}CSiMe_3)_4(PMe_3)_4$ and its isotopomers. The molybdenum complexes exhibit bands attributable to ν_a and ν_b; the frequencies of ν_a are roughly constant among these complexes ($SiMe_3$, 361 cm^{-1}; Me, 363 cm^{-1}; Bu^t, 359 cm^{-1}), while those for ν_b are more strongly alkynyl R-group dependent ($SiMe_3$, 398 cm^{-1}; Me, 386 cm^{-1}; Bu^t, 380 cm^{-1}). The spectrum of $Mo_2(C{\equiv}CBu^t)_4(PMe_3)_4$ additionally exhibits a band at 280 cm^{-1} that can be assigned to ν_c, which is strongly shifted from that of $Mo_2(C{\equiv}CSiMe_3)_4(PMe_3)_4$ (253 cm^{-1}), but that of $Mo_2(C{\equiv}CMe)_4(PMe_3)_4$ does not. For the latter compound, the 240−300 cm^{-1} region is a broad, undifferentiated signal that probably includes ν_c, $\delta(CPC)_{asym}$, and ν(MoP) modes. We have also tentatively assigned the alkynyl λ(CCC) modes of these complexes, but isotopic data would be required to confirm the assignments. The spectrum of $W_2(C{\equiv}CMe)_4(PMe_3)_4$ is very similar to that of the molybdenum analogue except that the relative intensity of the composite feature of the latter at ca. 350 cm^{-1} (ν_a and $\delta(CPC)_{sym}$) is greatly reduced for the tungsten compound, consistent with a shift in ν_a (the nominal metal−metal stretch) to lower frequency due to the mass effect. The frequency of $\nu(W_2)$ for $W_2Cl_4(PMe_3)_4$ has been assigned at 261 cm^{-1},[20] nearly coincident with $\delta(CPC)_{asym}$, but we do not observe significant differences in the 240−300 cm^{-1} spectral region between the molybdenum and tungsten propynyl derivatives that would allow assignment of this mode.

The FT-Raman spectra of $Mo_2(C{\equiv}CH)_4(PMe_3)_4$, $Mo_2(C{\equiv}CD)_4(PMe_3)_4$, and $Mo_2(C{\equiv}CH)_4(PMe_3\text{-}d_9)_4$ (Figure 9) are of

lower quality than those for $Mo_2(C{\equiv}CSiMe_3)_4(PMe_3)_4$ because samples decomposed upon extended irradiation at 1064 nm, even at very low laser powers. Nonetheless, it is clear from these spectra that the frequencies of the core modes differ significantly from those of the other $Mo_2(C{\equiv}CR)_4(PMe_3)_4$ (R = Me, Bu^t, $SiMe_3$) derivatives. Most striking is that there is not a band attributable to the nominal metal−metal stretch (ν_a) in the 350−360 cm^{-1} region; the only band in this region, at 357 cm^{-1}, exhibits a strong shift (−13 cm^{-1}) upon deuteration of the phosphine ligands and, thus, is attributable to the $\delta(CPC)_{asym}$ mode. Bands at 421, 387, and 299 cm^{-1} in the spectrum of $Mo_2(C{\equiv}CH)_4(PMe_3)_4$ are insensitive to phosphine deuteration but shift to lower frequency upon deuteration of the ethynyl ligand (Figure 9), so these bands are assigned as the analogues of ν_a, ν_b, and ν_c. The 387 cm^{-1} band (ν_a) undergoes the smallest shift upon ethynyl deuteration and, thus, presumably has relatively little ν(MoC) character. By inference, then, this band is assigned as $\nu(Mo_2)$ (ν_a). The large difference between its frequency and those of other $Mo_2X_4(PMe_3)_4$ complexes[10] is not expected on the basis of the metal−metal distance, however, which is nearly identical with those of other $Mo_2X_4(PMe_3)_4$ (X = halide) and $Mo_2(C{\equiv}CR)_4(PMe_3)_4$ complexes (Table 6). Bands arising from λ_{ip}(CCD) and λ_{op}(CCD) modes are clearly evident in the spectrum of $Mo_2(C{\equiv}CD)_4(PMe_3)_4$ at 494 and 476 cm^{-1}; by comparison, the frequency of λ(CCD) for $CH_3C{\equiv}CD$ is 497.5 cm^{-1}.[49] The corresponding bands in the spectrum of $Mo_2(C{\equiv}CH)_4(PMe_3)_4$ appear at 599 and 540 cm^{-1}, but are barely resolved due to the low signal-to-noise ratio; they are more clearly observed, at nearly identical frequencies, in the higher-quality spectrum of $Mo_2(C{\equiv}CH)_4(PMe_3\text{-}d_9)_4$. By comparison, the frequency of λ(CCH) for $CH_3C{\equiv}CH$ is 633.2 cm^{-1}.[49] The spectrum of $Mo_2(C{\equiv}CH)_4(PMe_3\text{-}d_9)_4$ exhibits well-resolved bands at 259 and 268 cm^{-1} that are assigned to $\delta(CPC)_{asym}$ and to a $\lambda(MoCC)_{asym}$ mode, respectively. Note that for the other compounds we have only assigned one band (ν_c) to a λ(MoCC) mode; a total of six such modes of this type are expected (Table 7), and since at least some of these may reasonably be expected in the 250−300 cm^{-1} region, our assignments in this region for all compounds but $Mo_2(C{\equiv}CSiMe_3)_4(PMe_3)_4$ are tentative.

Normal-Coordinate Calculations. Valence force-field normal-coordinate calculations at various levels of approximation were performed on $M_2(C{\equiv}CR)_4(PMe_3)_4$ complexes with the dual aims of quantifying the mixing among ν_a, ν_b, and ν_c that is clearly indicated by the resonance-Raman data for $Mo_2(C{\equiv}CSiMe_3)_4(PMe_3)_4$ and the FT-Raman data for $Mo_2(C{\equiv}CH)_4(PMe_3)_4$ and of assigning ν_c. Even with the extensive mode assignments provided by the FT-Raman spectroscopic studies of these complexes, however, there are far fewer observed frequencies than there are variables in these calculations; this required that various approximations be employed in the calculations, as is described in detail in the Experimental Section.

Given that the compound $Mo_2Cl_4(PMe_3)_4$ has a molecular structure that is quantitatively similar to those of the $Mo_2(C{\equiv}CR)_4(PMe_3)_4$ complexes and that its vibrational spectra are comparatively lacking in complexity, particularly regarding the nature of the core vibrational modes, we first performed valence force-field normal-coordinate calculations on $Mo_2Cl_4P_4$, where the PMe_3 ligand is approximated as a phosphorus atom, in order to establish benchmark force constants for use in the normal-coordinate calculations on $Mo_2(C{\equiv}CH)_4(PMe_3)_4$. The force field provided by these calculations is set out in Table 11. Due to the neglect of the phosphine methyl groups, the calculated f(MoP) and f(MoMoP) force constants are too small; thus, low-frequency (ν < 200 cm^{-1}) modes are not described well enough to allow detailed assignments of the spectra of $Mo_2Cl_4(PMe_3)_4$ to be made in this region based on the force field. The rationale for including a large number of force constants in the calculation was to probe the sensitivity of the frequencies and potential-energy distributions of ν_1 [a_1, $\nu(Mo_2)$] and the a_1-, b_2-, and e-symmetry ν(MoCl) modes to these low-frequency modes; fortunately, this sensitivity seems to be minimal. According to the PED the seven highest-frequency modes are the nine stretches (two of which are degenerate); the PEDs of the stretching modes correspond well to a previously presented valence-coordinate description of the motions.[20] Stretch−stretch and stretch−bend mixings are neither large nor sensitive to reasonable variations in the parameters. For example, increasing the mass of P in $Mo_2Cl_4P_4$ to that of PMe_3 while keeping all force constants the same shifts the calculated frequencies of ν_2 [a_1, ν(MoCl)] by −5 cm^{-1}, the frequencies of the b_2- and e-symmetry ν(MoCl) modes by less than −1.5 cm^{-1}, and the frequency of ν_1 [a_1, $\nu(Mo_2)$] by only −0.05 cm^{-1}.

To test whether the calculated force constants for $Mo_2Cl_4P_4$ are transferable to closely related molecules, vibrational frequencies were calculated for $Mo_2Br_4P_4$ and $Mo_2I_4P_4$ by changing the halide mass and scaling f(MoX) according to the calculated Au−X stretching force constants of *trans*-$[AuX_2(CN)_2]^-$ (X = Cl, Br, I),[22] which gave f(MoBr) = 1.156 and f(MoI) = 0.891 mdyn Å^{-1}; no other force constants, nor any geometrical parameters, were changed in these calculations. For $Mo_2Br_4(PMe_3)_4$, the calculated and experimental values are in good agreement: ν_1 [a_1, $\nu(Mo_2)$], calc = 352.8 cm^{-1} (obs = 352 cm^{-1}); ν_{10} [e, ν(MoBr)], 266.1 (264); ν_2 [a_1, ν(MoBr)], 158.3 (159); and ν_6 [b_2, ν(MoBr)], 189.2 (208). For X = I, the agreement is not as good: ν_1 [a_1, $\nu(Mo_2)$], 350.7 cm^{-1} (343 cm^{-1}); ν_2 [a_1, ν(MoI)] 110.0 (105); ν_6 [b_2, ν(MoI)], 156.0 (137). The calculation distributes ν_{10} [e, ν(MoI)] (experimental value of 177 cm^{-1}) over three e-symmetry modes at 240.9, 214.4, and 118.4 cm^{-1} (PEDs of 27.8%, 22.9%, and 36.6% ν(MoI), respectively). The degree of mixing of the e-symmetry stretching and bending modes is seriously overestimated in this calculation because MoI bending force constants (which should be considerably smaller than those for MoCl) were not adjusted and because of the considerable increases of the MoX distance (0.337 Å) and MoMoX angle (by 2.9°) of the iodo complex[10] relative to the $Mo_2Cl_4(PMe_3)_4$ structure[17] used for the calculation. Nonetheless, this strongly constrained calculation still gives semiquantitative agreement with experiment.[60]

In view of these comparisons, the calculated metal−metal force constant, $f(Mo_2)$ = 3.57 mdyn Å^{-1}, appears to be a general value for compounds of the $Mo_2X_4(PMe_3)_4$ class that have metal−metal bond distances of ca. 2.13 Å. That this force constant is nearly identical to that provided by the diatomic-oscillator approximation (3.56 mdyn Å^{-1})[10] is largely explained by the PED for this mode, which reveals it to be 86% Mo_2 in character (Table 11). Mixing of $\nu(Mo_2)$ and ν(MoX) stretching motions is small even for X = Cl, for which the stretching frequencies are closest (355 and 274 cm^{-1}, respectively) among the halides.

Valence force-field calculations have been previously reported on $Re_2X_8^{2-}$ (X = F, Cl, Br, I),[61−63] $Tc_2X_8^{n-}$ (X = Cl, Br; n = 2, 3),[63] $Os_2X_8^{2-}$ (X= Cl, Br, I),[63] "Mo_2O_8" (as a model for

(60) Because of the severe mixing among Mo−I stretching and bending modes that is indicated by the calculation, a fully adequate fit to the experimental spectra would require reoptimization of (at least) the eight force constants that involve halide motion; this is beyond the scope of this work.

Table 11. Results of Normal-Coordinate Calculation for $Mo_2Cl_4P_4$

	wavenumber (cm^{-1})		PED[a] (%)			
mode[b]	obsd[c]	calcd	$\nu(Mo_2)$	ν(MoCl)	ν(MoP)	bending contribution
ν_1 [a_1, $\nu(Mo_2)$]	355[d]	355.4	86.0	4.3	0.9	
ν_{10} [e, ν(MoCl)]	330[e]	330.2	0	85.9	0	
ν_6 [b_2, ν(MoCl)]	283[f]	286.2	0	91.6	4.7	
ν_2 [a_1, ν(MoCl)]	274[d]	270.1	0.1	88.4	11.4	
ν_7 [b_2, ν(MoP)]	(230)[g]	236.6	0	6.9	92.2	
ν_{11} [e, ν(MoP)]	230[f]	229.3	0	1.6	66.3	
ν_3 [a_1, ν(MoP)]	235[d]	225.2	0	17.6	82.3	
ν_{12} [e, δ(MoMoCl)]		165.4	0	6.9	26.5	δ(MoMoCl) (51.3)
ν_8 [b_2, δ(MoMoCl)]		132.7	0	5.8	4.4	δ(MoMoCl) (66.8)
ν_{16} [b_1, δ(ClMoP)]		126.8	0	0	0	δ(ClMoP) (100)
ν_{17} [a_2, δ(ClMoP)]		126.8	0	0	0	δ(ClMoP) (100)
ν_{14} [e, δ(ClMoCl)]		108.0	0	0.6	7.4	δ(ClMoP) (74.2)
ν_{15} [e, δ(PMoP)]		97.7	0	0.7	0	δ(ClMoP) (76.9)
ν_4 [a_1, δ(MoMoCl)]		94.1	14.5	4.6	0.3	δ(MoMoCl) (77.3%)
ν_9 [b_2, δ(MoMoP)]		78.6	0	0.1	5.4	δ(MoMoP) (62.8%)
ν_{13} [e, δ(MoMoP)]		74.2	0	0.1	5.6	δ(MoMoP) (76.2%)
ν_5 [a_1, δ(MoMoP)]		73.7	0	2.4	6.0	δ(MoMoP) (73.8%)

Valence Force Constants[h]

$f(Mo_2) = 3.574$ mdyn Å^{-1}
f(MoCl) = 1.386 mdyn Å^{-1}
f(MoP) = 0.756 mdyn Å^{-1}

f(MoMoCl) = 1.210 mdyn Å rad^{-2}
f(MoMoP) = 0.545 mdyn Å rad^{-2}
f(PMoCl) = 0.529 mdyn Å rad^{-2}

$f(Mo_2,MoCl) = 0.337$ mdyn Å^{-1}
f(MoCl,MoCl) = 0.068 mdyn Å^{-1}
$f(Mo_2,MoP) = 0.181$ mdyn Å^{-1}
f(MoP,MoP) = 0.223 mdyn Å^{-1}
f(MoCl,MoP) = 0.153 mdyn Å^{-1}
$f(Mo_2,MoMoCl) = -0.084$ mdyn rad^{-1}
$f(Mo_2,MoMoP) = 0.108$ mdyn rad^{-1}
f(MoCl,MoMoCl) = 0.142 mdyn rad^{-1}
f(MoP,MoMoP) = 0.179 mdyn rad^{-1}

[a] For conciseness, only the stretching contributions and the major bending contribution (when the latter is >50% of the PED) are tabulated. Mixing among bending internal coordinates is extensive in many of these modes. [b] Depictions of the modes according to this numbering are given in ref 20. [c] In addition to wavenumbers listed in this column, the following observed band wavenumbers (refs 10 and 20) were used as constraints in the final force-constant refinement: 181, 165, 153, 134, 131, 121, 108, and 86 cm^{-1}. [d] Reference 10. [e] Value for PEt_3 complex from ref 20. See this reference for discussion. [f] Reference 20. [g] Assumed value; see ref 20. [h] The metal−metal-torsion force constant (b_1 symmetry) was neglected. Force constants for ClMoCl and PMoP bending are not included in the calculation because these motions can be expressed as linear combinations of the other bending motions. In particular, the calculated e-symmetry modes at 108.0 and 97.7 cm^{-1} have PEDs corresponding to considerable δ(ClMoCl)/δ(PMoP) character.

$Mo_2(O_2CCH_3)_4$),[61] and $Mo_2Cl_8^{4-}$,[62] and the magnitudes of stretching and bending force constants arrived at in these earlier calculations are reasonably consistent with those reported here. Force constants for $Mo_2X_4P_4$ from a molecular-mechanics calculation have also been reported;[21] this calculation included repulsive terms in the potential, and therefore, the results are not directly comparable to the present force field, although stretching force constants from this prior study are, in fact, similar to our values. Valence force-field calculations for $Mo_2X_4(PMe_3)_4$ (X = Cl, Br, I) that treated only the three totally symmetric stretches (three symmetry force constants, no interaction force constants) have also been reported recently.[18] The Mo−Mo stretching force constants provided by those calculations (2.62−3.01 mdyn Å^{-1}) are much smaller than that reported here (3.57 mdyn Å^{-1}, Table 11); this results, in part, because the mixing between metal−metal and metal−halide stretching coordinates is calculated to be substantially greater in the three-mode force field[18] than in the present calculation. The nearly identical Mo−Mo distances and stretching frequencies for $Mo_2X_4(PMe_3)_4$ (X = Cl, Br) are reasonably interpreted in terms of the closely similar Mo−Mo force constants provided by the present force field, whereas in the three-mode force field the Mo−Mo force constants differ by 15% between these compounds.[18]

With the core force constants in hand from the $Mo_2Cl_4P_4$ calculation, valence force-field normal-coordinate calculations were performed on $Mo_2(C{\equiv}CH)_4P_4$. These calculations employed the metrical data available from the crystal structure of $Mo_2(C{\equiv}CH)_4(PMe_3)_4$[4] and estimates for Mo−C≡C−H force constants (see Experimental Section). The calculated frequencies and PEDs of the a_1-symmetry modes are set out in Table 12. The three highest-frequency modes (labeled i, ii, iii) are largely (≥85%) localized on the ethynyl ligands; these are the ≡CH (ν_{20}) and C≡C (ν_{19}) stretches and the C≡C−H bend (ν_{22}). The next three modes, iv, v, and vi, are in the frequency region for ν_a, ν_b, and ν_c. In marked contrast to $Mo_2Cl_4P_4$ (Table 11), for which $\nu(Mo_2)$ character is concentrated in a single a_1 mode, modes iv and vi of $Mo_2(CCH)_4P_4$ both have substantial $\nu(Mo_2)$ character (54.1% and 36.5%, respectively). The frequencies of these modes and of mode v, which has 2.9% $\nu(Mo_2)$ character, are calculated to shift significantly upon deuteration of the ethynyl ligand. Importantly, the $\nu(Mo_2)$ character of these modes is remarkably sensitive to isotopic labeling of the ethynyl ligand, with modes iv and vi dropping to 44.3% and 26.1% $\nu(Mo_2)$ character, respectively, and mode v increasing, 8-fold, to 23.6%. Although the calculated frequencies of modes iv, v, and vi are not in particularly good agreement with the observed frequencies of bands ν_a, ν_b, and ν_c, presumably as a result of the limitations of the calculation, the finding that these modes are strongly mixed is clearly in qualitative agreement with the experimental observations; the PEDs for modes iv, v, and vi indicate, then, that bands ν_a, ν_b, and ν_c be assigned to modes of strongly mixed $\nu(Mo_2)$, ν_{sym}(MoC), and λ_{ip}(MoCC) parentage. None of these

(61) Bratton, W. K.; Cotton, F. A.; Debeau, M.; Walton, R. A. *J. Coord. Chem.* **1971**, *1*, 121−131.
(62) Ketteringham, A. P.; Oldham, C.; Peacock, C. J. *J. Chem. Soc., Dalton Trans.* **1976**, 1640−1642.
(63) Preetz, W.; Peters, G.; Bublitz, D. *J. Cluster Sci.* **1994**, *5*, 83−106.

Table 12. Results of Normal-Coordinate Calculation on $Mo_2(CCH)_4P_4$.[a]

	wavenumber (cm^{-1})		calcd wavenumber shift (cm^{-1})		PED (%) for metal−metal coupled modes				
mode	obsd	calcd	$Mo_2(C{\equiv}CD)_4P_4$	$Mo_2(^{13}C{\equiv}^{13}CH)_4P_4$	$\nu(Mo_2)$	ν(MoC)	λ_{ip}(MoCC)	δ(MoMoC)	other
i	3269, 3242[b]	3255.0	−750.6	−16.2	0	0	0	0	ν(≡CH) (96.5)
ii	1909	1913.0	−104.1	−68.5	0	4.2	0	0	ν(C≡C) (91.9)
iii	599, 540	563.3	−75.1	−9.2	0.3	0.9	11.1	2.2	λ_{ip}(CCH) (85.3)
iv	421	386.1	−8.0	−2.7	54.1	17.6	8.4	12.3	
v	387	371.8	−17.5	−12.9	2.9	84.2	3.2	2.2	
vi	299	271.2	−23.0	−6.4	36.5	0.3	44.8	11.4	
vii	230	230.0	−0.1	−0.1	0.2	2.6	0	0	ν(MoP) (97.0)
viii	[c]	82.7	−4.8	−2.5	7.7	2.0	24.7	57.2	
ix	[c]	73.1	−0.5	−0.2	0	0.3	1.1	6.0	δ(MoMoP) (74.0)

Valence Force Constants[d]

f(C≡C) = 13.450 mdyn Å^{-1}
f(≡CH) = 5.650 mdyn Å^{-1}
f(MoC) = 2.000 mdyn Å^{-1}
f(C≡C,≡CH) = −0.150 mdyn Å^{-1}
f(C≡C,MoC) = 0.200 mdyn Å^{-1}
f(CCH) = 0.140 mdyn Å rad^{-2}
f(MoCC) = 0.260 mdyn Å rad^{-2}

[a] Only the nine a_1-symmetry modes calculated are given in this table. [b] Wavenumbers of ν(≡CH) for the PMe_3-d_9 derivative; these modes are obscured for the natural-abundance compound. Presumably, only one of these features corresponds to the a_1-symmetry mode. [c] Out of the observable range of our FT-Raman spectrometer. [d] Except for f(MoC) the optimized force constants from the $Mo_2Cl_4P_4$ calculation (Table 11) were transferred without change to this calculation, with C_α replacing Cl.

three modes is calculated to have significant MoP stretching or bending character. A very low frequency calculated mode, mode viii, has some $\nu(Mo_2)$ character, but it is better described as a mixed λ_{ip}(MoMoC) and λ_{ip}(MoCC) bend.

The mixing of modes iv, v, and vi (ν_b, ν_a, and ν_c) arises from two causes. First, f(MoC) is similar (ca. 2 mdyn Å^{-1}) to $f(Mo_2)$ (3.57 mdyn Å^{-1}), and the hypothetically unmixed (zero-order) a_1-symmetry ν(MoC) and $\nu(Mo_2)$ modes are expected to have very similar frequencies (350−400 cm^{-1}). Thus, these two stretching modes, with similar frequencies and force constants and a shared atom, will inevitably mix. Second, ν(MC) and λ-(MCZ) modes (where Z is an atom triply bonded to carbon) are typically strongly mixed by kinematic effects when symmetry allowed,[22−24] as is true for the a_1 modes in the present case. It is this latter aspect that most strongly differentiates these complexes from the $Mo_2X_4(PMe_3)_4$ (X = halide) derivatives. Small changes in any of the three important diagonal force constants have enormous effects on the PEDs, although effects on frequencies are smaller.[64] We have concluded that the calculated results, particularly the PEDs, are so exquisitely sensitive to small force-constant variations that meaningful refinements of our force field are not possible. That there is a large mixing of these three modes is, nonetheless, firmly established. It is noteworthy that the relatively large contribution of $\nu(Mo_2)$ to the highest frequency mode (ν_a) is entirely consistent with the vibronically resolved $^1(\delta{\rightarrow}\delta^*)$ electronic absorption band of $Mo_2(C{\equiv}CH)_4(PMe_3)_4$.[4]

To approximate the effect of terminal substitution of the alkynyl ligand we performed calculations in which the H atom was replaced by a C or Si atom, keeping all force constants unchanged. The three modes are still calculated to be mixed, but interestingly, $\nu(Mo_2)$ is more concentrated into a single mode, at 356.9 cm^{-1} (58.5% $\nu(Mo_2)$) for $Mo_2(C{\equiv}CC)_4P_4$ and 351.6 cm^{-1} (64.0% $\nu(Mo_2)$) for $Mo_2(C{\equiv}CSi)_4P_4$. Thus, heavy-atom terminal substitution of the alkynyl ligand reduces mixing, resulting in a purer (but still far from pure) $\nu(Mo_2)$ mode. The ν_a mode in $Mo_2(C{\equiv}CSiMe_3)_4(PMe_3)_4$ may therefore have more metal−metal stretching character than is indicated by the $Mo_2(C{\equiv}CH)_4P_4$ normal-coordinate calculation. Similarly, a calculation using the force field of $Mo_2(C{\equiv}CH)_4P_4$ but with the mass of the metal atom increased to that of W predicts $\nu(W_2)$ character to be concentrated (65.2%) in an a_1 mode at 234.2 cm^{-1}. Mixing between $\nu(W_2)$ and ν(WC) is negligible—an a_1 mode calculated at 372.4 cm^{-1} has 93.8% ν(WC) character—but there is significant mixing between $\nu(W_2)$ and λ_{ip}(WCC).

In contrast to the strong mixings among these totally symmetric core modes, their nontotally symmetric analogues are relatively pure. There are a total of 15 nontotally symmetric modes calculated below 600 cm^{-1}, all of which (except the torsion about the metal−metal axis) have a_1 counterparts with similar frequencies. Noteworthy among these are the ν(MoC) modes, which are calculated at 437.5 (e, 85% ν(MoC)) and 385.1 cm^{-1} (b_2, 95% ν(MoC)), respectively, for the natural-abundance compound.

It is important to note that the coupling among ν_a, ν_b, and ν_c does not significantly perturb the ν_{19} [a_1, ν(C≡C)] mode (Table 12), which is calculated to be 91.9% C≡C stretching in character. This is primarily due to the large energy mismatch (>1000 cm^{-1}) between ν(C≡C) and other totally symmetric core modes. Experimentally, a small splitting of the three ν-(C≡C) modes (a_1, b_2, e) of $Mo_2(C{\equiv}CSiMe_3)_4(PMe_3)_4$ (IR, 1991 (s); FTR, 1999 (vvs), 1995 (vvs, sh) cm^{-1}) is observed. The splitting can be reproduced in calculations by introducing an interaction force constant for the C≡C oscillators on a single metal center (1,1-Mo$(C{\equiv}C)_a(C{\equiv}C)_b$); the calculated value of this interaction constant ($f((C{\equiv}C)_a,(C{\equiv}C)_b)$ = 0.06 mdyn Å^{-1}; f(C≡C) = 14.08 mdyn Å^{-1}) is substantially smaller than *cis*-(C≡O,C≡O) interaction force constants (ca. 0.4 mdyn Å^{-1}) obtained using the Cotton−Kraihanzel model for ν(C≡O) vibrational modes of metal−carbonyl complexes.[65−67] The available data do not exclude the possibility of couplings between C≡C oscillators on adjacent metal centers, however.

(64) For example, increasing f(MoC) from 2.0 to 2.2 mdyn Å^{-1} in the calculation results in frequency shifts of iv, v, and vi of +8.8, +8.4 and 0.0 cm^{-1}, respectively; these small shifts correspond to the expectation that the frequency of an uncoupled ν(MoC) mode would increase by a factor of $(1.1)^{1/2}$ for such a force-constant change. However, there is a significant redistribution of the corresponding vibrational coordinates in the PEDs for iv and v, the $\nu(Mo_2)$ character for these modes changing from 54.1% and 2.9%, respectively, to 23.8% and 40.7%, respectively.

(65) Kraihanzel, C. S.; Cotton, F. A. *J. Am. Chem. Soc.* **1962**, *84*, 4432−4438.
(66) Kraihanzel, C. S.; Cotton, F. A. *Inorg. Chem.* **1963**, *2*, 533−540.
(67) Cotton, F. A. *Inorg. Chem.* **1964**, *3*, 702−711.

These three-bond (or four-bond) vibrational couplings are consistent with electronic interactions among the alkynyl units through the metal centers and, indeed, are hard to interpret in any other way, but it is difficult to say anything of a quantitative nature about the magnitude of these interactions.

Conclusion

This work demonstrates that the marked differences between the Raman frequencies and intensities of the $\nu(M_2)$ modes of $Mo_2(C{\equiv}CR)_4(PMe_3)_4$ complexes and those of $Mo_2X_4(PMe_3)_4$ (X = halide) complexes are due, primarily, to large kinetic mixing among the nominal $\nu(M_2)$, ν(MC), and λ_{ip}(MCC) modes of the dimetallatetraynes, rather than being a result of structural differences among these complexes. As a consequence of this mixing, we conclude that the unusual $\nu(M_2)$ frequencies and resonance-Raman intensity patterns found for these compounds[2,4] do not necessarily imply either unusual metal−metal force constants or electronic conjugation effects. In contrast, the ν(C≡C) modes of these complexes are highly C≡C localized; thus, the ν(C≡C) vibronic progressions observed in the $\delta{\rightarrow}\delta^*$ electronic transitions of $Mo_2(C{\equiv}CSiMe_3)_4(PMe_3)_4$ and $[Mo_2(C{\equiv}CSiMe_3)_4(PMe_3)_4]^-$ reflect C≡C excited-state distortions and, therefore, electronic delocalization across the $\delta/\delta^*(M_2)$ and π/π^*(C≡C) orbitals.[6]

The coupling between the ν(MC) and λ_{ip}(MCC) modes of the $M_2(C{\equiv}CR)_4(PMe_3)_4$ complexes is of the same general type as that present in mononuclear metal complexes containing multiply bonded ligands such as CO,[68,69] CN^-,[22−24,70] NO,[71] and NCX^- (X = O, S, Se).[72,73] Thus, it is reasonable to expect that such stretch−bend mixing will also be observed for binuclear complexes containing these ligands. One likely example of this is provided by a recent resonance-Raman study of $[Mo_2(CN)_8]^{4-}$, in which resonance enhancement (upon excitation within the $^1(\delta{\rightarrow}\delta^*)$ band) of bands at 309, 383, and 411 cm^{-1} is observed; all three bands have similar resonance-Raman excitation profiles.[74] These bands were assigned as δ(MoMoC) (equivalent to λ_{ip}(MoMoC) in this paper), ν(MoC), and $\nu(Mo_2)$, respectively. The close correspondence in frequency between these bands of $[Mo_2(CN)_8]^{4-}$ and bands ν_a, ν_b, and ν_c for $Mo_2(C{\equiv}CR)_4(PMe_3)_4$ complexes is quite striking. Our results suggest that similar three-mode interactions are operative for $[Mo_2(CN)_8]^{4-}$, and that normal-coordinate calculations on this ion would reveal that these modes have parentages more complex than the proposed[74] first-order assignments.

Acknowledgment. Support to K.D.J. through Lubrizol and Andrew W. Mellon graduate fellowships and to R.F.D. and M.A.V. from the Haines Research Fund at Wabash College is gratefully acknowledged. This research was generously supported by the National Science Foundation through Grants CHE-9307013 and CHE-9700451.

Supporting Information Available: An X-ray crystallographic file, in CIF format, for $M_2(C{\equiv}CMe)_4(PMe_3)_4$ (M = Mo, W), $Mo_2(C{\equiv}CSiMe_3)_4(PMe_3)_4$, and $Mo_2(C{\equiv}CBu^t)_4(PMe_3)_4$ is available on the Internet only. Access information is given on any current masthead page.

IC980866U

(68) Jones, L. H.; McDowell, R. S.; Goldblatt, M.; Swanson, B. I. *J. Chem. Phys.* **1972**, *57*, 2050−2064.
(69) Jones, L. H.; McDowell, R. S.; Goldblatt, M. *Inorg. Chem.* **1969**, *8*, 2349−2363.
(70) Jones, L. H.; Swanson, B. I.; Kubas, G. J. *J. Chem. Phys.* **1974**, *61*, 4650−4655.
(71) Jones, L. H.; McDowell, R. S.; Swanson, B. I. *J. Chem. Phys.* **1973**, *58*, 3757−3770.
(72) Schmidt, K. H.; Müller, A.; Chakravorti, M. *Spectrochim. Acta* **1976**, *32A*, 907−915.
(73) Forster, D.; Horrocks, W. D. *Inorg. Chem.* **1967**, *6*, 339−343.
(74) Bell, I. M.; Clark, R. J. H.; Humphrey, D. G. *J. Chem. Soc., Dalton Trans.* **1997**, 1225−1229.